Study Report SR488 [2025]

Energy performance of innovative water heating technologies

Stephan Rupp, Roman Jaques, Michael Lanner and Andrew Pollard

BRANZ
1222 Moonshine Rd, RD1, Porirua 5381
Private Bag 50 908, Porirua 5240
New Zealand
branz.nz

ISSN: 1179-6197

Preface

This report compares a select number of promising new, easily retrofittable water heating technologies. These water heating systems make use of photovoltaic panels to supplement or replace the usual reticulated energy requirements. The promising technologies are compared to the most common water heating systems operating in homes (single element hot water cylinder) and also the most efficient current technology (split air-to-water heat pump). Various hot water draw-off profiles are assessed to better understand the energy performance characteristics of these technologies and utility provided. The practical implications of retrofit are also discussed. The results of this report could be used as the basis for considering the financial returns possible with these different types of water heating systems.

Acknowledgements

We would like to thank the project's advisory group – their input is greatly appreciated:

- Rod Miller (Plumbing, Hydraulics and Drainage Consulting Ltd) representing New Zealand Master Plumbers.
- Nikki Buckett (Kāinga Ora), representing public housing and urban developers via KiwiBuild Unit and Housing New Zealand.
- Christian Hoerning (MBIE) representing central government and building system performance.
- James le Page (Consumer NZ) representing consumers, specifiers and designers.
- Adrian Kerr (Temperzone) representing interests in renewable energy, energy efficiency, low-carbon technologies.

Energy performance of innovative water heating technologies

BRANZ Study Report SR488

Authors

Stephan Rupp, Roman Jaques, Michael Lanner and Andrew Pollard

Reference

Rupp, S., Jaques, R., Lanner, M., & Pollard, A. (2025). *Energy performance of innovative water heating technologies* (BRANZ Study Report SR488). BRANZ Ltd.

Abstract

In the last 10 years, several new innovative low-carbon residential water heating technologies have been developed that show promise. In this report, solar direct photovoltaic (PV) water heating and CO_2 heat pump water heating are examined.

Solar direct PV systems use a small PV array connected directly to a hot water cylinder via a simple controller/modifier. They differ from whole-house PV systems in their size, complexity and cost.

The other technology examined for this report are CO_2 heat pump water heaters. While heat pump water heaters have been around for some time, using CO_2 as the refrigerant has a number of advantages, including improved efficiency and performance.

This project took an experimental approach, examining three solar direct PV water heating systems of varying sizes and one CO_2 heat pump water heater system and compared each of these with a reference system of an electric resistance storage water heater. These systems were installed at BRANZ and were tested over winter and summer seasons with small and large test draw-off schedules.

All of the systems were effective in reducing the grid electricity required to provide for the hot water demand when compared to the reference system but the savings varied depending on the system, the season and the draw-off scenario.

The outputs of this project could be used as part of a cost-benefit analysis of these types of water heaters.

Keywords

Innovative water heating, photovoltaic-assisted water heating, direct PV, heat pump water heating, low-carbon water heating, water heating performance.

Contents

Figures

Tables

Executive summary

In the last 10 years, several new innovative low-carbon residential water heating technologies have been developed. These systems show promise to greatly reduce the carbon, energy and lifetime costs compared to the more traditional water heating.

Three different direct solar photovoltaic water heating systems and one CO_2 heat pump water heater system were examined and compared with a traditional electric resistance storage hot water system. These systems were installed at BRANZ and were tested over winter and summer with small and large water draw-offs.

All of the systems examined were effective in reducing the grid electricity required but the savings varied depending on the technology involved, the size of the system, the season and the amount of water used.

The CO_2 heat pump water heater was the most consistent-performing system requiring less than half (36–46%) of the grid electricity as a traditional electric resistance water heater regardless of the time of the year.

All the direct PV systems performed well in summer. Even with a small system and a large water draw-off, only about one-third of the energy requirements were needed to be sourced from grid electricity.

The PV systems were less effective in winter. If a large amount of hot water is to be provided by the system, a larger system would reduce the amount of grid electricity the system would require.

The outputs of this project could be useful for as inputs into an analysis of the costs and benefits from these types of water heaters.

1. Introduction

In New Zealand, there are approximately 1.9 million households (Stats NZ, 2023), each requiring some form of water heating using around 31% of New Zealand's residential energy (EnergyConsult, 2020). Water can be heated with a range of technologies – gas, electrical resistance heating, heat pumps, solar thermal or solid fuels. Hot water systems in New Zealand have traditionally been electrically heated storage cylinders. The BRANZ Pilot Housing Survey (White, 2020) found that 73% of household hot water systems were electric storage systems. There has been a shift away from electric storage heating to instant gas heating systems (Figure 1).

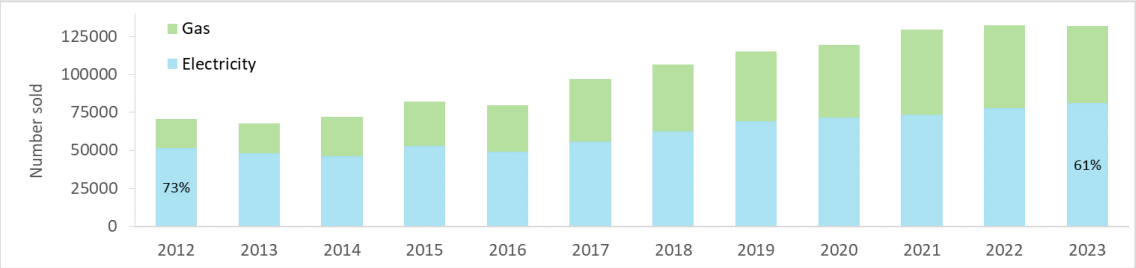

Figure 1. Sales figures for electric storage cylinders and instant gas hot water systems (EECA, 2023).

Water heating can be a substantial contribution to evening peak demand (Dortans et al., 2019). Managing when hot water is heated would provide a means to reduce the stress on power networks. Ripple control, a demand management technology that enables consumers' electrical equipment to be switched off and on using a remote signal (EECA, 2020), has been used throughout the country. It has been relied upon as the main demand management tool since the 1950s. This provides electricity distribution businesses the ability to cut off up to approximately 15% New Zealand's annual peak demand. About half of New Zealand's households have this feature.

In the last 10 years, several new innovative low-carbon residential water heating technologies have been developed[1] that show promise to greatly reduce the carbon, energy and lifetime costs of the more traditional systems. If used more widely, there is considerable potential for these new lower-carbon replacement technologies to benefit consumers, electricity distribution businesses and the environment. Most of these innovative systems focus on what is informally named as solar direct PV and are the focus of this BRANZ study. These solar direct PV systems utilise a small PV array (typically in the range of 1–3 kW and independent from the grid) connected to a simple controller/modifier to maximise the energy being fed directly into a hot water cylinder heater element. A recent magazine article has featured these types of water heaters (Turner, 2023).

Note that these direct PV systems are different from the more complex and expensive solar diverter systems. Diverter systems use surplus electricity from an existing rooftop solar system to heat water and don't have a dedicated set of PV panels powering them. In direct PV systems, if there is not enough sun, grid electricity is used to boost the heating element, which is kept on a separate circuit (Figure 2). These systems usually have a two-element system where grid electricity needed for topping up the water temperatures to 60°C charge the top element where hot water is drawn.

[1] For example, www.arrayenergy.com.au/products/sun-flux-ii and www.nexol-ag.net.

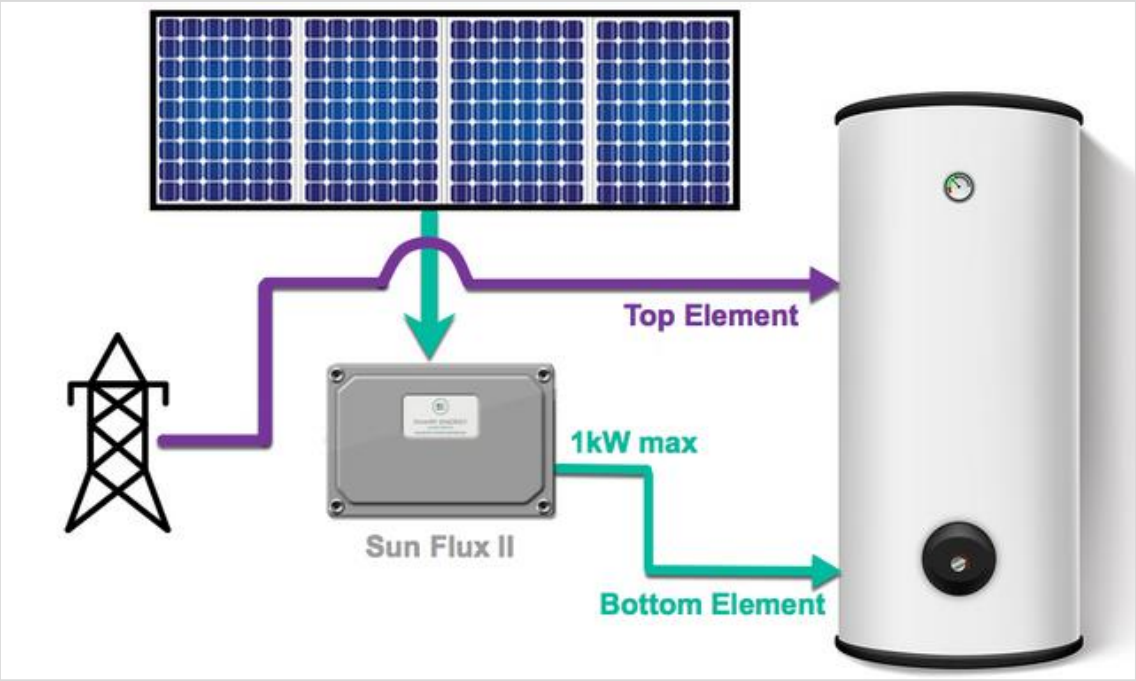

Figure 2. Schematic of a direct PV system with dual heating elements – Sun Flux example (SolarQuotes, 2017).

PV direct systems enable zone heating of the tank in layers to minimise grid consumption. When there is low solar radiation, the system prioritises the upper zone to reheat first via the grid. Once the upper zone has reached its target temperature of 60°C, the system switches to the lower heating element.

Compared to the more traditional solar thermal supplementary hot water systems, PV direct systems have many advantages, including:

- flexibility in terms of where the collector is in relation to the water store as only electricity is being transported
- no plumbing challenges such as having to penetrate the roof, transport pressurised hot water or periodically check and recharge with anti-freeze (typically glycol)
- a very simple electrical-only set-up
- lower overall cost due to the simplicity of the control/photovoltaics/wiring needed
- lower ongoing maintenance as no extra management is needed when occupants away, there are and no issues with extreme weather events (such as hail) or accidental impact due to the robustness of the PV panels, which have performance guarantees for 25+ years, and there are no moving parts
- no coordination of multiple trades for installation as only electrical work is required.

This project seeks to compare these new water heating systems to current best-case technologies (the highest performing air-sourced heat pumps available) for the New Zealand context. It also seeks to understand the potential for these new technologies to impact New Zealand's upcoming international carbon commitment obligations,[2] infrastructure costs due to peak loading (lines companies and end users), fuel poverty (national equity) and national energy security (reducing reliance on non-renewable energy sources).

[2] Under the Paris Agreement, Aotearoa New Zealand has set a Nationally Determined Contribution of reducing net emissions by 50% below gross 2005 levels for the period 2021–30.

Clearly, no domestic water heating system is without an environmental impact when examined over its lifetime, no matter the energy source or how efficient it is. The focus of this report is restricted to the operational energy use of the water heater.

1.1 Background

There is very little information on the seasonal or annual performance of PV direct water heating devices. The closest information available relates to solar thermal systems, which, although related, are distinctly different in their energy conversion, energy transport and system control.

In order to fill this knowledge gap, five identical 250 L hot water cylinders were set up at the BRANZ campus within an existing test building, each with dual heating elements. Three cylinders were set up with a selection of direct PV solar controls from REFUsol (German developed), Sun Flux (Australian developed) and Easy Warm (New Zealand developed). The fourth system utilised a split CO_2 refrigerant air-to-water heat pump solution from Reclaim (Japanese developed) still with a 250 L cylinder. The fifth set-up was the reference system comprised of a 250 L cylinder driven entirely from grid electricity. Details on the individual systems are given in section 2.3.

Each system was tested using a range of hot water usage profiles to emulate a household for weeks at a time. By measuring the energy provided to the system and the temperature increase of the water, the efficiency of each system under a variety of loads and draw-offs was calculated to enable the five systems' performance to be assessed and directly compared.

1.2 Methodology overview

An experimental approach using largely off-the-shelf hot water cylinders was chosen. Although the novelty of some of these studied systems does not put them beyond sophisticated simulation techniques, it was felt that the complexity, especially of the PV systems, justified collecting experimental data that will be useful not only to better understand these systems but also to benchmark simulation studies in the future.

A simple/direct comparison between the various hot water systems examined here is not the aim of the study nor is it possible. Each of the three innovative direct PV technologies had different specification requirements in terms of ideal energy collectors and control set-up. For instance, the three PV array sizes ranged from 1.2–3.2 kW_{peak}. One PV system can be used to retrofit a single-element HWC, while the other two generally require a second resistive element. The heat pump system was likely to perform more economically when using high hot water draw-off profiles. Consequently, the comparisons rely on metrics that normalised these differences benchmarked against a traditional, single-resistive element reliant on grid-electricity exclusively.

The goal was to operate the systems with minimal human intervention or setting adjustment throughout the year. It was assumed this would best reflect the 'set and forget' scenario common for water heaters in homes. As an example, the Sun Flux has the option of manually switching between solar or grid electricity input to a single resistive element. While this is a potential retrofit option for a single-element cylinder, this was deemed unpractical for the average consumer and not tested here. Thus, this system was tested on a dual heater element cylinder. The exception to this 'set and forget' system is the Easy Warm system, which allows some control of the grid-electricity input. By utilising this control feature there is potential to significantly boost the performance over a no-intervention setting. This is discussed in detail below.

Several experiments (with as identical settings as practical) were conducted on a seasonal basis to test system performance across all four seasons. Although the climatic conditions (specifically solar irradiance and temperatures) vary, the controlled experimental set-up means they vary equally for all systems so useful comparative performance data can be derived. Various daily and seasonal hot water draw-off schedules and thermostat settings were conducted over extended periods to capture a range of solar irradiation conditions.

Draw-off profiles should ideally be based on realistic typical household quantities rather than current methods that are largely unrelated to actual household usage (Pollard, 2010). In terms of recent findings, there is no single source of draw-off profile that can be used as a basis for testing or modelling (EECA ,2021). Fortunately, using desktop simulation, it has been found that the pattern for a given total hot water draw-off doesn't have a large impact on the efficiency or performance of the hot water heater.

For this study, the seasonal draw-off profiles were based on the four daily energy draw-off schedules set out in AS/NZS 4234:2021 *Heated water systems – Calculation of energy consumption* – 52 MJ/day (large), 39 MJ/day (medium), 25.6 MJ/day (small) and 17.1 MJ/day (very small) – and varied according to the month (see Table B.6.3 in AS/NZS 4234:2021).

For this study, these monthly variations were adjusted to enable a greater number of experiments under more similar conditions. This daily load profile is divided into 10 draw-off events spread over the day. An example for the small daily load of 25.6 MJ/day is shown in Table 1.

Table 1. Hourly energy draw-off schedule – small daily load.

NZ Peak Daily Thermal Energy Load			Daily Load Profile (Small Daily Load)					
Large [MJ/day]	Medium [MJ/day]	Small [MJ/day]	Hour	Hourly Load Factor	Energy Winter [MJ]	Energy Spring [MJ]	Energy Summer [MJ]	Energy Autum [MJ]
52.0	39.0	25.6	00:00					
			01:00					
			02:00					
Seasonal Load Profile			03:00					
Month	Load - Standard	Load - Implemented	04:00					
			05:00					
December	0.65		**06:00**	**0.05**	1.28	1.06	0.74	0.91
January	0.51	**0.58**	07:00					
February	0.58		**08:00**	**0.16**	4.10	3.40	2.38	2.91
March	0.60		09:00					
April	0.72	**0.71**	**10:00**	**0.15**	3.84	3.19	2.23	2.73
May	0.83		11:00					
June	0.89		**12:00**	**0.11**	2.82	2.34	1.63	2.00
July	0.99	**1.00**	13:00					
August	1.00		**14:00**	**0.08**	2.05	1.70	1.19	1.45
September	0.90		15:00					
October	0.83	**0.83**	**16:00**	**0.07**	1.79	1.49	1.04	1.27
November	0.76		17:00					
			18:00	**0.11**	2.82	2.34	1.63	2.00
			19:00					
Energy [MJ/Hour] =			**20:00**	**0.13**	3.33	2.76	1.93	2.36
Daily Load x	Seasonal Load x	Hourly Load Factor	21:00					
			22:00	**0.11**	2.82	2.34	1.63	2.00
			23:00	**0.03**	0.77	0.64	0.45	0.55
			SUM =	1	*25.6*	*21.2*	*14.8*	*18.2*

The BRANZ experiments were conducted using the small energy draw-off profile and the large energy draw-off profile. Previous BRANZ work (Isaacs et al., 2010; Pollard, 2010) has indicated that low draw-off volumes may be more reflective of the actual New Zealand practice. However, it is important to use a large draw-off contrast to examine the impact of households with higher than average hot water use.

Since the instrumentation necessary to safely record the heater power was beyond the scope of this project, no detailed comments can be made on the efficacy of the three PV control units themselves (i.e. the ratio of the DC input power to the power delivered to the resistive element).

2. Experimental equipment

This section describes the individual components of each hot water storage system in detail. General components used throughout the project are described in section 2.1 with the system control and data acquisition software briefly described in section 2.2. The five individual hot water storage systems are introduced in detail in section 2.3. The experiments themselves and results are described and analysed in section 3.

2.1 System components

2.1.1 PV modules

All three PV hot water systems use identical solar panels – REC N-PEAK BLK2 produced by REC.[3] The cells and modules are manufactured in Singapore. The PV panels are made from 120 half-cut,[4] n-type monocrystalline silicon cells. Electrical specifications at standard test conditions (STC)[5] and nominal operating conditions (NOCT)[6] are given in Table 2.

Table 2. PV module specifications.

Electrical parameter	Values at STC	Values at NOCT
Nominal power P_{MPP}	315 W_p	238 W_p
Nominal voltage V_{MPP}	33.9 V	31.4 V
Nominal current I_{MPP}	9.31 A	7.56 A
Open circuit voltage V_{OC}	40.5 V	37.5 V
Short circuit current I_{SC}	10.09 A	8.07 A

As discussed in section 1.2, the number of panels and their configurations (series or parallel connection) varied between the systems. The direct PV systems' string layouts (collection of panels or arrays) with their respective electrical characteristics are shown in Table 3. The range of total power for each system ranged from 1.2–3.1 kW_p.

Table 3. PV module layouts.

System	String layout	Electrical characteristics – strings (at STC)
1. REFUsol	3 strings with 2 modules connected in parallel each – 6 modules in total	String 1/1: 630 Wp, V_{mpp} = 33.9 V, I_{mpp}=18.6 A String 1/2: 630 Wp, V_{mpp} = 33.9 V, I_{mpp}=18.6 A String 1/3: 630 Wp, V_{mpp} = 33.9 V, I_{mpp}=18.6 A Total: **1,890 W_p**
2. Sun Flux	1 string with 4 modules in series	String 2: **1,260 W_p**, V_{mpp} = 135.6 V, I_{mpp} = 9.3 A
3. Easy Warm	1 string with 10 modules in series	String 3: **3,150 W_p**, V_{mpp} = 339 V, I_{mpp} = 9.3 A

In total, 20 panels were installed at an inclination of 16° on a north-facing roof at BRANZ's Judgeford test site and fixed approximately 50 mm above the long-run metal roof cladding using an aluminium rail system to allow for good ventilation (Figure 3).

[3] REC Corporation, Norway – www.recgroup.com.
[4] Cut 156 mm² cells in half to reduce resistive losses by boosting voltage and reduce current.
[5] Irradiance = 1,000 W/m², air mass AM = 1.5, temperature = 25°C.
[6] Irradiance = 800 W/m², air mass AM=1.5, temperature = 20°C

Figure 3. Solar PV panels installed on BRANZ test building.

2.1.2 Pyranometer

The global irradiance on a horizontal surface was measured in close proximity to the PV array using a Delta-T[7] SPN1 pyranometer. In addition, a Hukseflux instrument was installed recording the global, horizontal irradiance.

2.1.3 Hot water cylinders

Five 250 L mains pressure hot water cylinders were set up, each with two heating elements. Manufactured in Christchurch by Superheat, they are factory fitted with 3 kW elements and are 560 mm in diameter and 16,00mm tall. Apart from a built-in access port for the vertical temperature probe, their construction was standard. The standard resistive elements are controlled by bimetal actuated and spring-loaded thermostats[8] mounted to the outside of the inner cylinder vessel. The adjustable range is 50–70°C.

The heat pump-powered hot water cylinder also used a 250 L Superheat cylinder. A Reclaim Energy CO_2 hot water heat pump was used for comparative purposes. This is a split system with an outdoor compressor and an indoor hot water cylinder.

When installed, thermal imaging was used to check heat losses to the immediate environment. As can be seen in Figure 4, significant thermal losses were immediately obvious around connections, anode and heater element pocket. Standing losses were calculated as approximately 70 W for each cylinder.

Three were set up with a selection of PV solar solutions from REFUsol, Sun Flux and Easy Warm. Another system utilised a Reclaim Energy CO_2 heat pump. One was a reference cylinder driven entirely by grid power.

[7] Delta-T Devices, UK– www.delta-t.co.uk.
[8] Robert Shaw, USA – www.robertshaw.com.

Figure 4. Hot water cylinder with thermal image overlays of connection points to the cylinder and temperature scale on right-hand side.

2.1.4 Thermocouples/PRT sensors

Each cylinder was fitted with 6 K-type thermocouples recording the temperatures within six equally sized 'stacked' water zones. This was achieved by inserting six braided thermocouples vertically from the top of each cylinder through an additional top port. Each thermocouple was made to a different predetermined length coinciding with the respective subzone being measured.

The inlet water temperature was measured by a Pt100 platinum resistive thermometer (PRT) mounted directly to the inlet copper pipe inside the building. Before any readings were taken for relevant energy calculations, the pipe was flushed for several minutes to avoid overestimating the water temperature.

2.1.5 Water flow meters

The five individual water flow meters were installed on the cold-water inlet side of the systems to avoid problems with the potentially very hot water. A pulsed output was provided upon water flow, which was captured by our data acquisition system. The devices were calibrated to 36 pulses/L and the flow was approximately adjusted with a manual valve to yield 20 L/min during a hot water draw-off episode.

2.2 Data acquisition and software

2.2.1 FlexiDAQ (LabVIEW)

Data acquisition of all parameters as well as control of the automated water draw-off was achieved with BRANZ's in-house software package FlexiDAQ written using LabVIEW.

2.2.2 DC transducers

DC voltages and currents of the PV strings were measured using an Agilent 34940A multiplexer unit. Due to the different grounding states of the heater units, it was necessary to electrically decouple the PV power side from the measurement side. This was achieved by using DC voltage and current transducers.

It is important to note that the PV power measurement was performed on the input side of heater devices of systems 1–3. As internal losses could not be captured for these devices, this measurement is an overestimate of the total energy supplied to the resistive heater element in the cylinder.

2.3 Whole-system description

The following sections describe the systems as a complete assembly. No tempering valve (mixing hot and cold water to achieve a desired water temperature) was installed on the hot water outlet of any of the systems as the water meters needed to capture exclusively the water that entered the hot water cylinder. Apart from this, the remainder of the plumbing installation was according to code.

2.3.1 System 5. Reference

The reference system (Figure 5) was a standard resistive element hot water system. Two elements were installed for consistency with the other units but only the bottom element was connected to the electricity grid and was sized at 3 kW. The cylinder was made from stainless steel with a nominal capacity of 250 L. Actual usable volume was measured to be closer to 240 L, which was subsequently used for the analysis.

Figure 5. Reference system.

The cylinder had an additional access port at the top for inserting the thermocouple rod with has six sensors. The sensors were spaced so that each thermocouple recorded the temperature in a 40 L volume.

This system was used to estimate the standing losses for this type of cylinder. Without any water draw-off, the thermostat was set to T = 60°C, yielding an average temperature throughout the cylinder of 57.9°C. This setting was maintained for 7 days with the room temperature conditioned to T = 15°C. The average daily electrical energy supplied to the heater element was measured as 7.9 MJ/d (2.2 kWh/d). The standing losses under these conditions were then obtained as 92 W. No special efforts had been made to install additional insulation around pipes and ports other than an insulated sleeve around the hot water pipe. The intention was to reproduce a more realistic New Zealand household scenario.

2.3.2 System 1. REFUsol

The REFUsol/AE PV heater uses the direct current produced by PV modules to heat the water (Figure 6). Unlike the other two direct PV-powered systems, which can be operated on standard heater elements, the REFUsol unit has a proprietary heater element (consisting of three independent resistive heaters) and control system. To accommodate the proprietary element, the cylinder had to be manufactured with a slightly larger threaded port.

Figure 6. REFUsol controller (red unit) with DC cables from the three PV strings connected to the unit.

The specification recommends a maximum of 2.7 kW_{peak} of PV power, while the stated heating power output is 1.5 kW. As stated in Table 3, three strings with a nominal power output of 630 W_p each were installed. As shown in the Appendix B, the maximum power used to heat the water was limited to the stated 1.5 kW, even when the PV system could provide more energy.

The three independent PV strings were independently controlled by three maximum power point trackers (MPPTs). This would benefit installations where the three PV strings could not be installed on the same roof orientation but needed to be installed on parts of the roof with different orientations.

Excess electricity cannot be redirected to other uses and ends up as wasted heat in the panels and the system electronics. The system is functional in a blackout situation, which may provide some resilience in emergencies. The power output of the PV strings is measured on the input side to the device. This is the case for all three PV systems. The actual energy input to the heater element after losses in the device itself is not captured. The efficiency of the REFUsol unit is given to be above 99%. Cooling of the power electronics is achieved by natural convection. However, there are no large external cooling fins, indicating small operational losses.

It is German made and produced since 2014 by AEI Power GmbH.

2.3.3 System 2. Sun Flux

The Sun Flux PV controller (Figure 7) is marketed as an innovative, high-quality solar hot water controller and described as an off-grid/hybrid solar controller with up to 96% peak efficiency and requiring no plumber to install. It can accept 2–6 solar panels (up to 1.6 kWp capacity) supplying/powering up to a maximum of 1.5 kW to the element. As detailed in Table 3, the four panels installed for this system have a nominal power output of 1.26 kWp under standard test conditions. It does not function with an MPPT but uses an alternative insulated-gate bipolar transistor for modified DC output.

Figure 7. Sun Flux controller (black unit) top left.

Excess power is wasted – it cannot be redirected to other end uses. It is functional in a blackout situation.

The unit can also be connected to the household electricity grid so that the PV system can be bypassed using a manual switch to choose between the grid or the solar system as the energy source to a single resistive heater element. In theory, this system is then capable of being used as a retrofit to a single heater element hot water system. The grid electricity function was not used in our set-up and the unit always only supplied solar energy into the bottom heater element, while the top element is connected to the electricity grid.

It is manufactured by Sharp Energy in Australia.

2.3.4 System 3. Easy Warm HOT PV/EnaSolar

The Easy Warm Hot PV system uses a variable output voltage inverter (EnaSolar) together with a controller to provide solar hot water (Figure 8). The 3.8 kW inverter model was chosen (maximum usable DC input power 4 kW), which is larger than the nominal output power of the PV array to stay within the limits of the 3kW resistive heater element. It has one MPPT for the solar array.

Figure 8. Easy Warm system with EnaSolar inverter.

It is potentially the easiest of the three direct PV systems to add on to an existing house, requiring no changes to existing plumbing and no additional pipework. The system can be retrofitted to an existing hot water cylinder with a single heater element. The controller can be programmed to feed grid electricity into the heater element when the PV array is insufficient – two time windows for each day of the week can be programmed. It also offers a manual boost mode.

In order to avoid wasted electricity generation potential during times when the cylinder is at its maximum temperature, the operating manual suggests installing a second grid-tied inverter together with the non-grid-tied inverter used to power the resistive hot water cylinder element. This grid-tied inverter would feed electricity into the household grid or the wider electricity grid. However, such an approach seems to be an unjustifiable technological redundancy.

It is functional in a blackout situation.

When purchased, this was a New Zealand designed and made (essentially a modified EnaSolar/Enatel inverter) system. It has been manufactured since 2014.

It is the most complex but flexible of the three direct PV systems.

2.3.5 System 4. Heat pump

The air-to-water heat pump system chosen was a Reclaim Energy CO_2 hot water heat pump, one of the few CO_2 refrigerant systems available in New Zealand (circa 2021). It is Japanese made and has been manufactured since 2003. Cold water is taken from the bottom of the cylinder (the white pipe in Figure 9) and pumped to the outside unit where it is heated and returned to the top of the cylinder. No resistive heater element is utilised.

Figure 9. Cylinder used with the Reclaim Energy CO_2 heat pump system.

The outdoor unit was ground mounted with minimum pipework between the compressor and cylinder to optimise performance (Figure 10). It is a single pass system especially chosen for its low global warming coefficient refrigerant (CO_2), which is often overlooked in the pursuit to lower environmentally impacting water heating specification.

Figure 10. Reclaim Energy CO_2 outdoor unit.

Reclaim Energy CO_2 units are advertised as being super-efficient with a coefficient of performance of 5 and suitable for and New Zealand climate conditions.

Note that the Reclaim Energy CO_2 heat pump is designed to be connected to a 300 L hot water cylinder to store adequate amounts of hot water. Thus, the results using a 250 L cylinder might reflect less than optimum performance characteristics. However, this was compensated for by the study's indoor location of the cylinder unit, which are specified to be used outside where it would incur much higher heat losses.

The Reclaim Energy CO_2 smart controller enables some customisation so that homeowners can set the system to operate in parallel with their PV system or at a time when electricity companies offer the cheapest tariffs (Apricus, n.d.).

3. Results

To assess the performance of the hot water systems, a series of four experiments were undertaken. These experiments varied two factors likely to be most influential in the performance of the hot water systems – the volume of the hot water drawn-off from the system (large or small) and the season (summer or winter). Each experiment ran over a 2–3-week period, which allowed for a variation in daily irradiation to be included. As the experiments had to be run sequentially, it was necessary to do some of the summer testing in late spring and some of the winter testing in autumn. System performance was compared between each innovative system and the reference system rather than between the innovative systems themselves.

3.1 Spring – small draw-off

All systems were tested for 20 consecutive days in November 2021 applying the small energy load from Table 1 together with the seasonal factor of 0.83 (Table 4).

Table 4. Experiment summary: spring – small draw-off.

Experiment period (Exp009)			Spring: 11–30 November 2021 (20 days)		
Load/hot water energy draw-off			Small: 21.25 MJ/day		
System	**Lower element**		**Upper element**		**Comments**
	Temperature	Source	Temperature	Source	
1. REFUsol	70°C	Solar panels	60°C	Electricity grid	
2. Sun Flux	70°C	Solar panels	60°C	Electricity grid	
3. Easy Warm	70°C	Solar panels	Not connected		No grid power window defined
4. Heat pump	60°C				
5. Reference	60°C		Not connected		

The daily nominal draw-off was 21.25 MJ. The upper booster element (grid powered) was activated for the REFUsol and Sun Flux systems. (The Easy Warm system had an upper resistive element installed but this was not connected.) The thermostat temperature was set to T_{upper} = 60°C for these upper elements. The thermostat for the lower PV-powered element was set to T_{lower} = 70°C for PV systems 1–3. The higher-than-normal temperature setting for the PV-powered elements ensured the highest possible energy storage provided by the solar panels. The Easy Warm system had no grid booster time window defined so no grid power was used during this experiment. The heat pump system and the reference system (bottom element thermostat) were set to maintain a temperature of 60°C consistent with typical practice.

3.1.1 Spring irradiance results

Figure 11 compares the daily global horizontal irradiance measured at BRANZ, Judgeford, during the time of the experiment with average historical NIWA data for Kelburn, Wellington, approximately 25 km away. The data is given as a statistical box whisker plot on the left – the coloured boxes represent 25% to 75% quartiles with the whiskers indicating maximum and minimum. The white bar indicates median values while the black line gives mean values. The NIWA data is obtained by averages of each hour of the day in November using 18 years of climate data. These historical hourly averages are then summed for each day. The Judgeford daily irradiance values are given on the graph on the right.

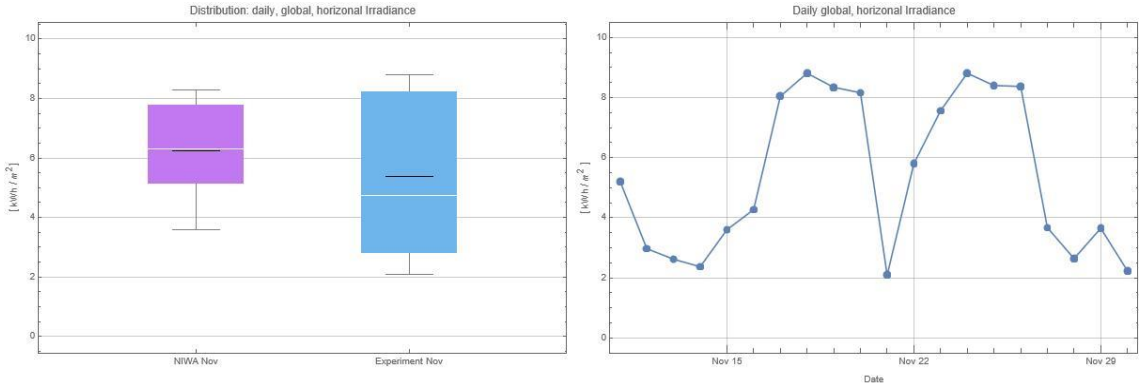

Figure 11. Irradiance for spring experiment.

The average irradiance during our experiment was noticeably lower compared to the long-term NIWA average. Several overcast days reduced the experimental site's global, horizontal, daily irradiance sum to an average of 5.3 kWh/m² in comparison to the historical 6.3 kWh/m² NIWA average. Thus, the experimental conditions were slightly disadvantageous, and the spring performance of the solar systems would be further improved by more representative irradiation conditions.

3.1.2 Spring comparison: 1. REFUsol to 5. Reference

The REFUsol system easily fulfilled the performance criterion of maintaining the upper two cylinder volumes above 50°C at all times. Figure 12 shows the temperatures in the REFUsol system on 19 November 2021 for each of the six cylinder sub-zones.

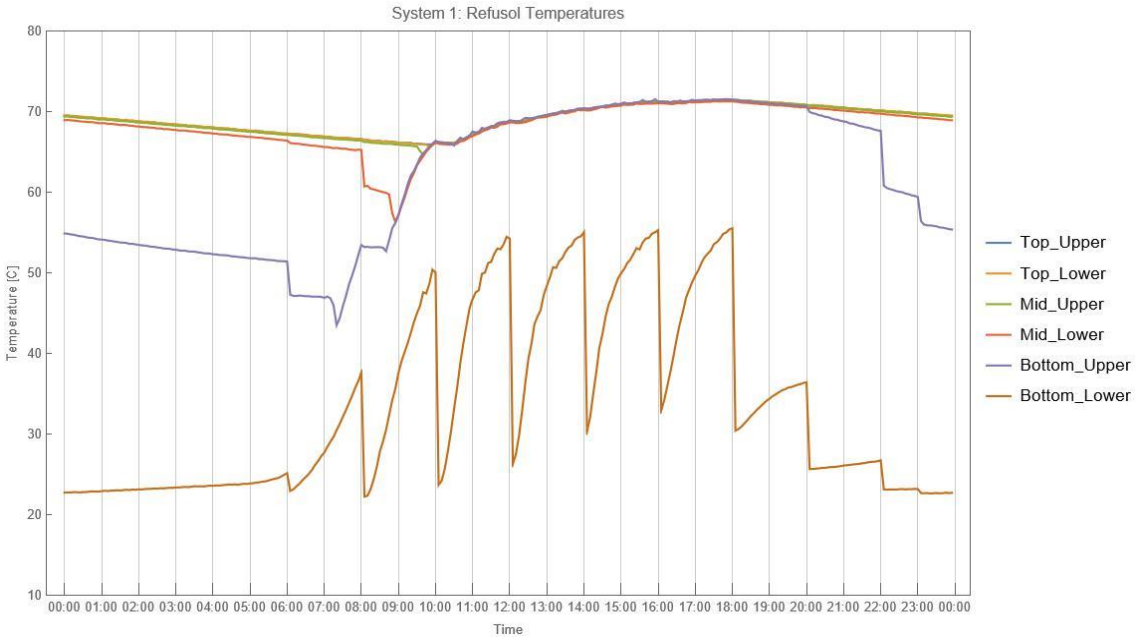

Figure 12. Temperature and total energy – REFUsol system – 19 November 2021.

The water draw-off episodes are clearly visible as cold water enters the bottom of the cylinder causing a temperature drop, which is captured by the lower thermocouples. While the temperature drop during the draw-off cycles is visible for the lowest two thermocouples in the morning and evening periods, only the lowest thermocouple senses the draw-off episodes during the peak sunshine hours. The energy provided by the solar panels on this sunny day is sufficient to quickly heat the bottom volume of

water. The temperature in the top half of the cylinder never drops below approximately 65°C, therefore the grid-powered top resistive element is not activated. The maximum temperature reached in the cylinder is just above 71°C. Thus, the entire energy need (cylinder losses plus water draw-off) is provided by the solar PV panels. The energy figures at the start and at the end of the day are nearly identical at around 333 MJ.

While the REFUsol system shows a highly dynamic distribution of temperatures during a day, the conventional reference system (Figure 13) has a much more homogeneous temperature distribution. Only the very bottom volume deviates significantly from the T = 60°C thermostat setting due to water draw-off and energy losses. The reference system heating element is switched on 10 times during the day, correlated to the draw-off episodes, while the REFUsol system does not need any grid energy on this sunny spring day.

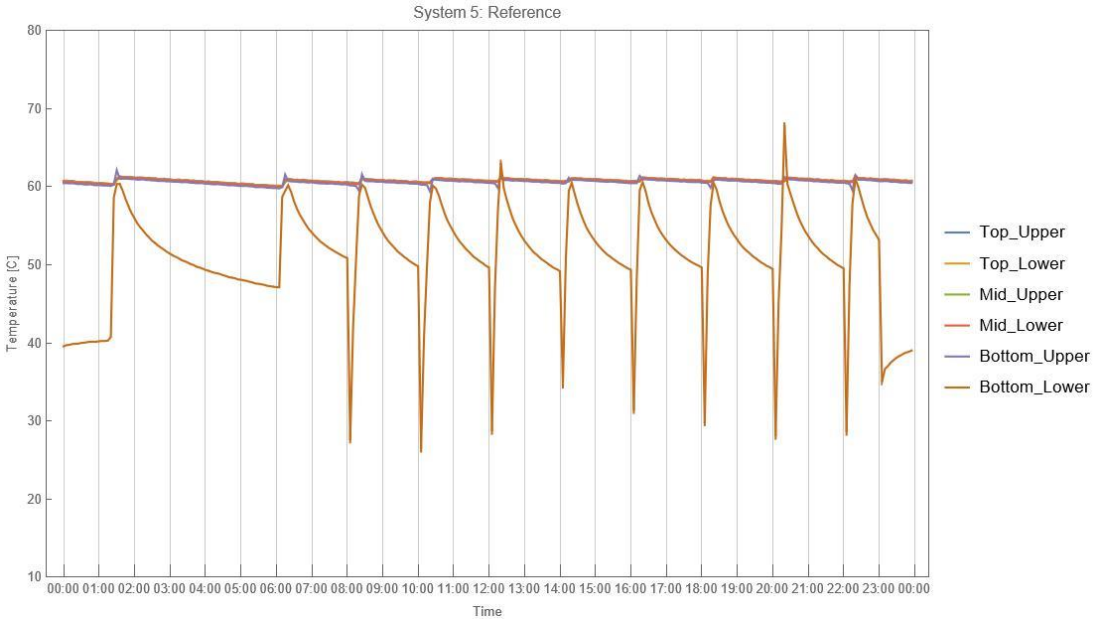

Figure 13. Temperature – reference system – 19 November 2021.

Overall, the average daily grid energy input to the reference system was 30.3 MJ/d (8.4 kWh/d). This is a consistent result with an average measured daily hot water draw-off of 22.1 MJ/d (6.1 kWh/d) plus the previously measured standing losses of a cylinder of 7.9 MJ/d (2.2 kWh/d) when the cylinder water temperature is maintained at 60°C.

In contrast, the REFUsol system had a slightly higher average daily energy draw-off of 22.7 MJ/d. The hot water energy draw-off (plus the standing losses) was predominantly met by the PV panels: the average, daily energy generated by the six solar panels was 25.4 MJ/d. Seven out of the 20 spring days saw the upper grid-connected element contributing to the energy demand. The largest daily demand from the grid was 15.3 MJ/d. Not surprisingly, the demand for grid electricity correlated with days of lower solar irradiance. The total energy demand of the REFUsol system was 335 MJ at the start of the experiment but only 320 MJ at the end of the 20-day period due to the irradiance conditions. To correct for this, we assumed that an additional 15 MJ needed to be provided by the grid. With this correction, the average daily grid energy required over the 20 days of the experiment was 3.6 MJ/d.

The standing losses of the REFUsol during operation were different compared to the very homogeneous reference system. While the top half of the cylinder sees higher temperatures and therefore larger energy losses, the lower half of the cylinder has long periods with temperatures below 30°C with correspondingly smaller losses.

In summary for this spring experiment, for a small draw-off, we found that the conventional reference system used an average of approximately **30.3 MJ/d (8.4 kWh/d)** of grid electricity, while the REFUsol system used approximately 12% of this with a grid electricity demand of around **3.6 MJ/d (0.9 kWh/d)**.

3.1.3 Spring comparison: 2. Sun Flux to 5. Reference

The Sun Flux system also achieved the criterion of the top two cylinder volumes never dropping below 50°C during this experiment. The measured average daily hot water draw-off was 22.1 MJ/d, the same as for the reference system. The average daily energy generated by the four PV panels over the 20 days was 17.8 MJ/d. The power generated by these four panels was not enough to cover the drawn-off hot water (standing losses in addition) and, as expected, the upper grid-connected element was activated. Again, correcting for the reduced total hot water energy in the cylinder at the end of the experiment as compared to the start, the daily average energy drawn by the upper element was 10.6 MJ/d. The need for the grid-connected element to be activated was seen in 18 out of the 20 days.

Figure 14 shows the temperature and total energy of the Sun Flux system on a sunny spring day. The maximum temperature reached during the day was 63°C at around 16:00. There was only one occasion on this day where the Sun Flux system activated the top grid element at around 11:50.

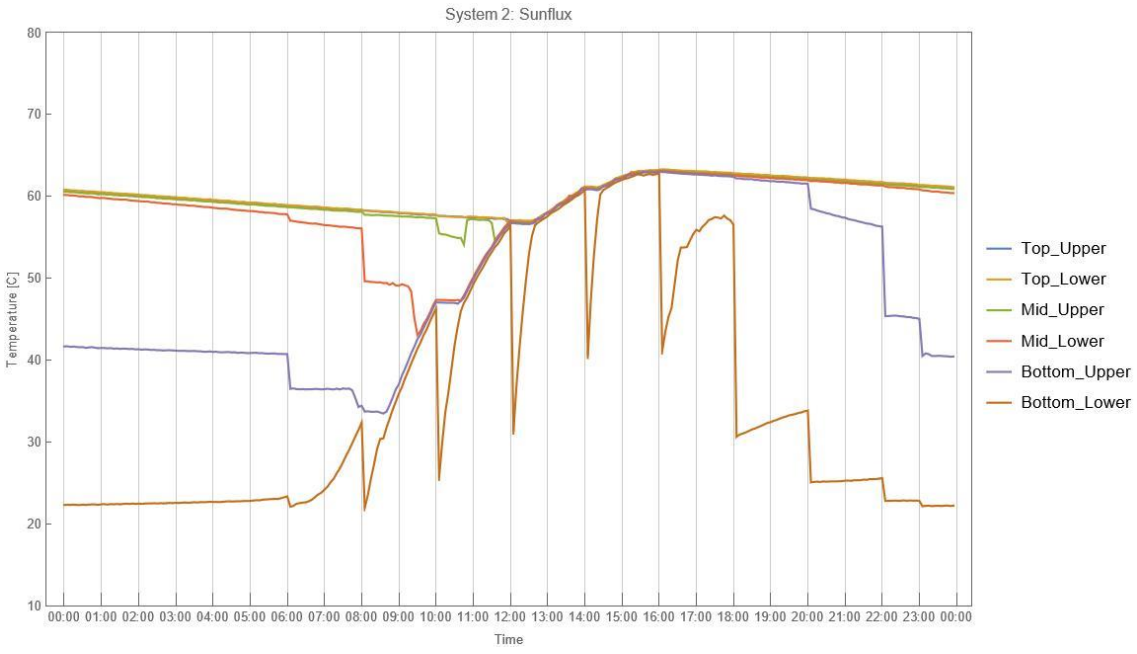

Figure 14. Temperature and total energy – Sun Flux system – 19 November 2021.

Comparing the necessary grid imported energy of the conventional reference system of 30.3 MJ/d (8.4 kWh/d), the Sun Flux system required only around 33% of the reference system grid energy – **10.6 MJ/d (2.9 kWh/d)**.

Comparing the REFUsol system and the Sun Flux system, Figure 15 shows the necessary grid electricity as a function of the daily irradiation. The approximate daily energy removed from the cylinders (hot water draw-off plus standing losses) is indicated by the red data point on the y-axis. While there is a trend visible for the Sun Flux system, the data is significantly scattered especially for the REFUsol system.

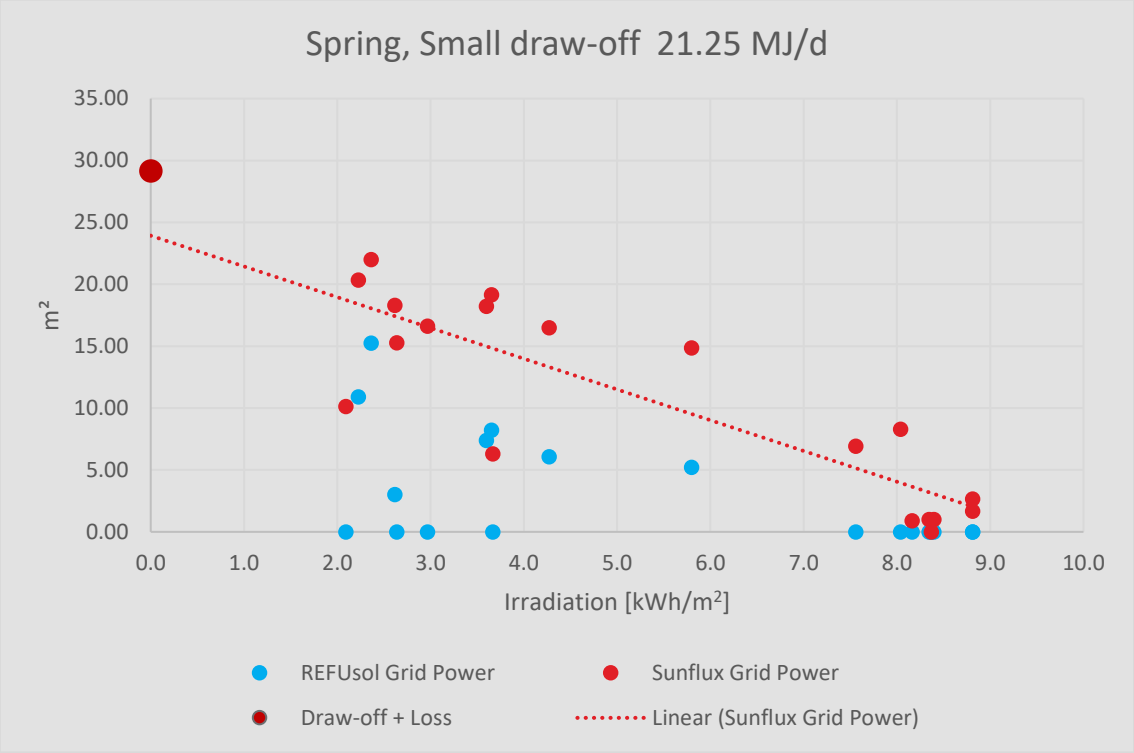

Figure 15. Comparison of REFUsol and Sun Flux systems.

This is a result of the generally low grid power figures for this small draw-off in spring and the energy stored in the cylinder – a very sunny day will leave the entire volume of the cylinder at a high temperature. If this sunny day is followed by an overcast day, the low water draw-off will leave the bottom part of the cylinder at a colder temperature. However, the top half might still be hot enough not to switch the grid-power heater. As a consequence, a low irradiation day might see no grid power required. The correlation between irradiance and grid power will be more pronounced at higher draw-off patterns.

Above approximately 6 kWh or daily irradiance, the REFUsol system would not require any grid electricity for this small draw-off scenario.

3.1.4 Spring comparison: 3. Easy Warm to 5. Reference

With its 10 solar panels, the Easy Warm system is the most powerful of the three PV systems. The resistive heater element can be powered by either the solar panels or the electricity grid by defining a maximum of two operational time windows for each day of the week where a switch changes the input from the solar power inverter to the electricity grid. For this spring experiment, this option was not used – all the power was sourced exclusively from the solar panels. As mentioned above, this switch makes the system the only option for retrofitting existing hot water cylinders with only one resistive element. (As mentioned above, while the Sun Flux system also has the option of operating one single element, this is a manual switch and deemed unpractical for

most applications.) The Easy Warm system is also the only one that converts the direct current output from the PV panels to a true sine curve of 50 Hz. This conversion is inevitably responsible for some electrical losses, and the unit has extensive cooling fins that at times become quite hot. Since we only measured the electrical energy output from the solar panels and not the energy that was actually arriving at the heating element, the PV energy output is an overestimation.

The Easy Warm system easily achieved the criterion of the top two cylinder volumes never dropping below 50°C during the experiment. The Easy Warm system had a slightly higher average daily energy draw-off of 22.9 MJ/d compared to the reference system (22.1 MJ/d). The average daily energy produced by the 10 panels was 32.4 MJ/d. Assuming a daily approximate energy loss of 7.9 MJ, the energy generated by the solar panels exceeded the sum of energy drawn off plus standing losses. No grid electricity was used at all. The cylinder had a net energy content of 331 MJ at the end of the experimental period, slightly down from the 335 MJ at the start of the period. Consequently, the grid energy requirements were adjusted to 0.2 MJ/day.

Figure 16 shows the temperatures as recorded in the six cylinder volumes from top to bottom as well as the time-dependent total stored energy in the cylinder. Even without any grid electricity, the upper volumes of the cylinder reach the maximum thermostat setting of around 70°C. The recovery of the temperature of the bottom-most volume, after hot water was withdrawn during the daytime, was very quick. It took less than 30 minutes until the set temperature of 70°C was reached again.

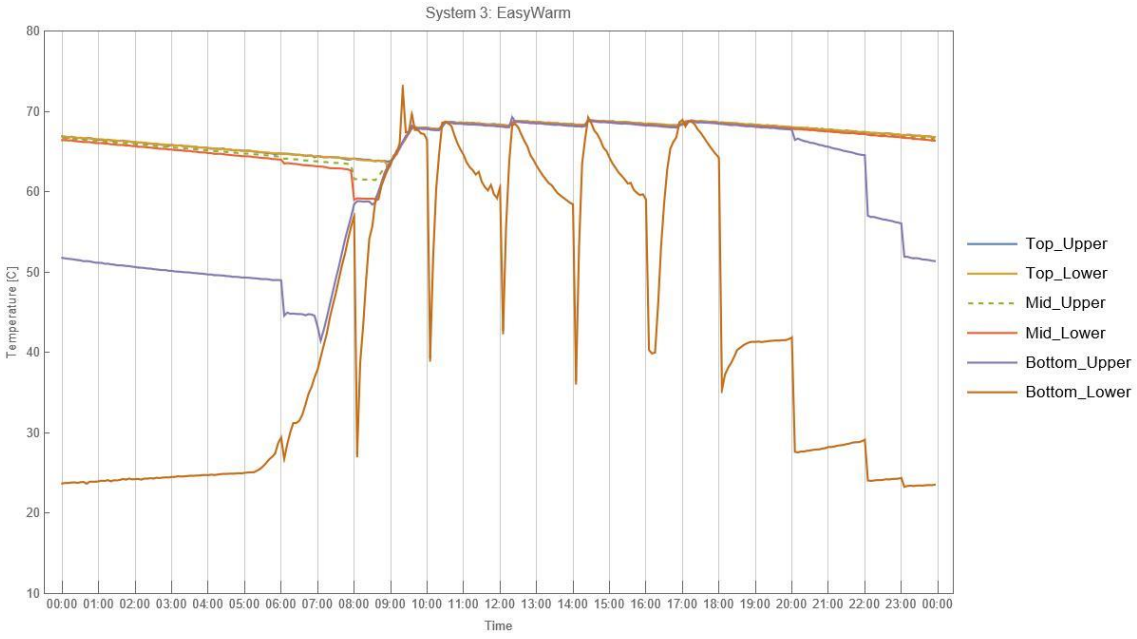

Figure 16. Temperature and total energy – Easy Warm system – 19 November 2021.

We chose to install a number of solar panels close to the nominal input capacity of the inverter, which is good practice to optimise the efficiency of the complete system. This larger number of panels easily achieved the hot water needs during the experimental period. However, with this larger array of solar panels, it was difficult to avoid periods where energy could not be stored the cylinder (even at a 70°C thermostat setting). Inevitably, during such periods, energy generation potential is wasted.

Figure 17 shows the measured power output of the 10 solar panels of the Easy Warm system for 19 November 2021 – a sunny day with some cloud cover in the morning

and late afternoon. Approximately 33 MJ (9 kWh) was generated on the input side of the inverter by the panels and used to heat the water. On the other hand, approximately 48 MJ (13 kWh) potential energy generation was wasted with three periods between 10:30 and 16:00 where the system did not utilise the solar energy.

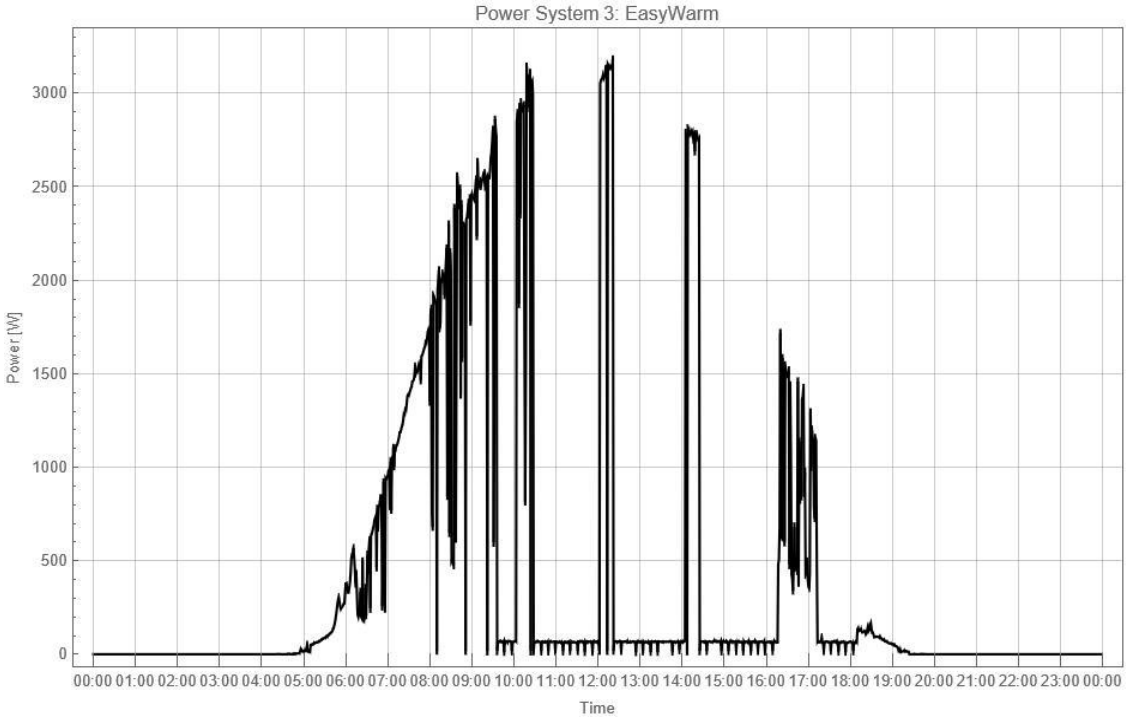

Figure 17. PV power output – Easy Warm system – 19 November 2021.

3.1.5 Spring comparison: 4. Heat pump to 5. Reference

Temperature dynamics in the heat pump cylinder (Figure 18) are noticeably different from the solar powered systems due to the latter's energy input during daylight hours.

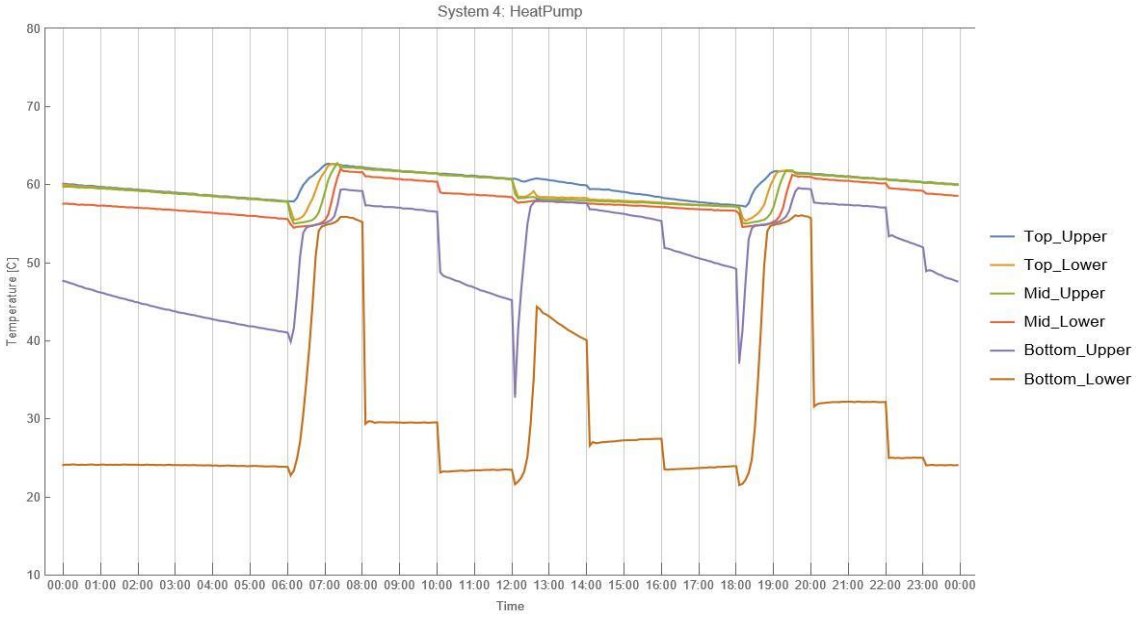

Figure 18. Temperature – heat pump system – 19 November 2021.

In the case of the heat pump set-up, the water draw-off episodes are noticeable in the bottom and mid-zone thermocouples. The draw-off episodes at t = 6:00, 12:00 and 18:00 triggered the heat pump unit to start circulating and heating the water.

The average, daily energy drawn-off as hot water was 22.2 MJ/d and very similar to the other systems. Adding an approximate 7.9 MJ/d of standing losses, the total energy removed from the cylinder was again around 30 MJ/d as expected. This standing loss figure of 7.9 MJ/d is however an underestimate for this particular system since water (hot or warm) is pumped from the cylinder to the outside unit and back. While the pipework is insulated, significant losses are likely to occur here.

The average daily grid energy required to operate the system was measured to be **12.0 MJ/d (3.3 kWh/d)**, which is less than half of the figure of energy being removed from the hot water tank. The difference is energy extracted from the surrounding air by the heat pump. While this experiment was not intended to estimate a coefficient of performance, we found that, under these conditions, an electrical input energy of 12 MJ would result in a heating energy input of 30 MJ. Recalling the daily energy needed for the reference system of 30.3 MJ/d (8.4 kWh/d), the heat pump system offers significant energy savings – it requires only 39% of the energy used by the reference system.

3.2 Summer – large draw-off

It can be assumed that all PV systems with the same small hot water draw-off schedule would perform similarly or better in summer with its higher insolation levels. As the performance was satisfactory for all systems, the nominal hot water draw-off was increased to 30.2 MJ/d for the summer experiment. Otherwise, the parameters were unchanged as summarised in Table 5.

Table 5. Experiment summary: summer – large draw-off.

Experiment period (Exp010)			Summer: 18 December 2021 – 9 January 2022 (23 days)		
Load/hot water energy draw-off			Large: 30.16 MJ/d		
System	**Lower element**		**Upper element**		**Comments**
	Temperature	Source	Temperature	Source	
1. REFUsol	70°C	Solar panels	60°C	Electricity grid	
2. Sun Flux	70°C	Solar panels	60°C	Electricity grid	
3. Easy Warm	70°C	Solar panels	Not connected		No grid power window defined
4. Heat pump	60°C				
5. Reference	60°C		Not connected		

3.2.1 Summer irradiance results

The average irradiance during the summer experiment was somewhat larger compared to the long-term NIWA average (Figure 19). There was only one short period of low sunshine at the end of December. The daily average irradiance was recorded at 7.3 kWh/m² for the experiment in comparison to the historical 6.5 kWh/m² NIWA average. Thus, unlike the spring period, the experimental conditions were slightly advantageous. The summer performance of the solar systems would be slightly reduced by more representative irradiation conditions.

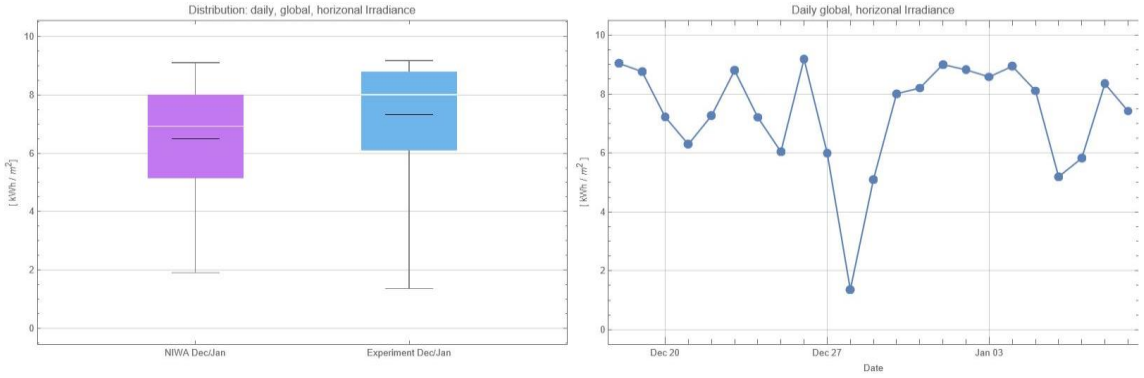

Figure 19. Irradiance for summer experiment.

3.2.2 Summer comparison: 1. REFUsol to 5. Reference

At no time over the experimental period did the temperature drop below 50°C in the upper two water volumes of the REFUsol system (Figure 20). The average daily hot water draw-off for the REFUsol system was 31.5 MJ/d as compared to 30.9 MJ/d for the reference system. The average daily grid electricity input into the reference system was 38.5 MJ/d (10.7 kWh/d), which is consistent with the hot water draw-off energy and the measured standing losses. The latter was lower than the measured 7.9 MJ/d as the ambient temperature in the building was higher in the summer period.

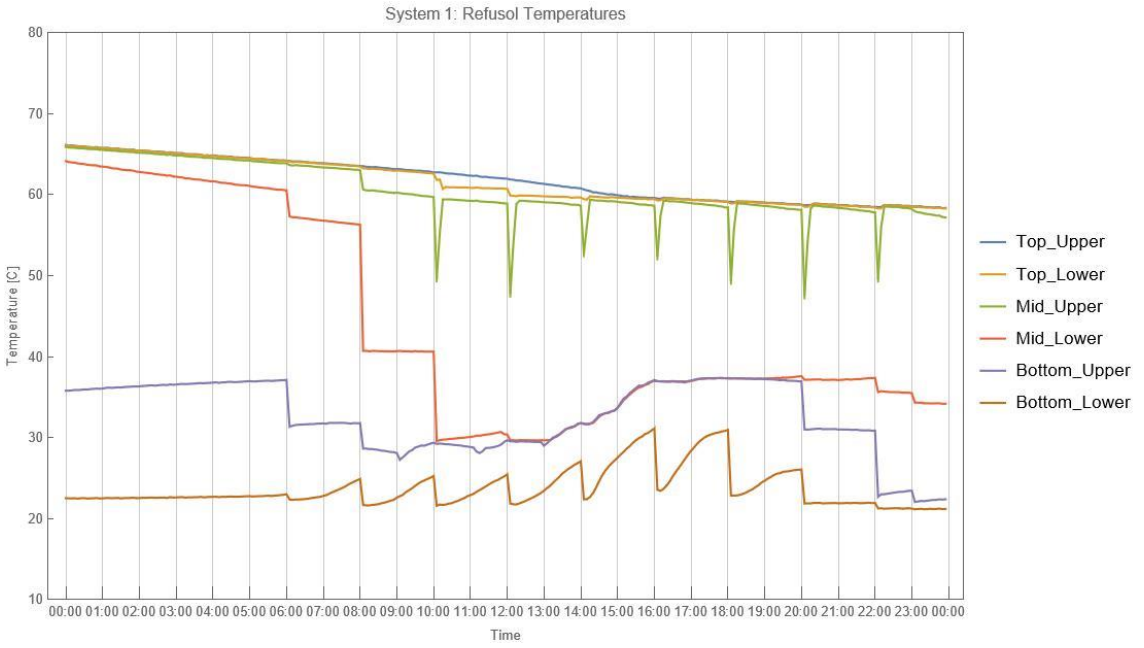

Figure 20. REFUsol temperatures during an overcast day – 28 December 2021.

The total stored energy in the REFUsol system was lower at the beginning of the experiment as compared to the end by 5 MJ. This was not corrected to stay conservative. The average daily energy provided by the six solar panels was 36.1 MJ/d. Out of the 23 days of this summer experiment, 13 days did not require any electricity drawn from the grid, while 10 days saw energy demands between 1.3 MJ/d and 14.9 MJ/d. The daily average grid energy demand for the REFUsol was **1.8 MJ/d**. Adding the energy provided by the PV system to the grid energy consumed (36.1 + 2 MJ/d = 38.1 MJ/d), we arrive again at a figure close to the hot water draw-off plus the approximated loss value (31.5 + 7.9 MJ/d = 39.4 MJ/d).

Figure 20 shows the temperatures in the REFUsol system during the worst performing day during the summer experiment. Clearly visible are the water draw-off events and the seven times when the upper grid-connected element was powered (green thermocouple). The top half of the cylinder was maintained around T = 60°C, mainly by grid power. The lower half of the cylinder essentially acted as a 'warm reservoir' for feeding the upper cylinder volume. There was a significant temperature difference between the two volumes. The solar system was still able to lift the minimum temperatures over midday hours to around 30°C.

Comparing the reference system with its **38.5 MJ/d (10.7 kWh/d)** grid electricity demand, we found the REFUsol system required only approximately 5% of the energy used by the reference system to achieve a comparable hot water supply under a high draw-off scenario over the summer months. As expected, this was an improvement on the 12% value found for the spring small draw-off scenario.

3.2.3 Summer comparison: 2. Sun Flux to 5. Reference

At no time over the experimental period did the temperature drop below 50°C in the upper two water volumes of the Sun Flux system.

The average daily hot water draw-off for the Sun Flux system was 30.9 MJ/d, the same as for the reference system. The PV panels delivered an average daily energy yield of 24.6 MJ/d. The daily average grid power need was **13.0 MJ/d**. The total daily approximate energy input was then 37.6 MJ, which is again balanced by the hot water draw-off and the approximate standing losses.

The average daily grid electricity input into the reference system was **38.5 MJ/d (10.7 kWh/d)**. Thus, the Sun Flux system required only approximately 34% of the energy used by the reference system to achieve a comparable hot water supply under a high draw-off scenario over the summer months.

3.2.4 Summer comparison: 3. Easy Warm to 5. Reference

The Easy Warm system failed to maintain the criterion of the top two cylinder volumes not dropping below 50°C on two overcast days. However, the system was set up not to use any grid power with a high draw-off scheme. As such, failing this criterion on two out of 23 days is not surprising. Manual intervention by the householder (activating the boost mode) would have quickly rectified this shortfall. The alternative of having daily time windows defined where grid power is switched on avoids manual interventions.

The daily average hot water draw-off was measured as 31.6 MJ/d. The average daily PV energy output into the inverter was 41.6 MJ/d, thus providing for all the energy removed from the cylinder (hot water draw-off and losses). The difference in the energy balance is explained to some degree by the inverter losses. The cooling fins of the inverter were found to get hot during the daily operation.

3.2.5 Summer comparison: 4. Heat pump to 5. Reference

Higher draw-off scenarios should lend themselves to higher efficiencies of the heat pump system as compared to the PV systems. The additional, non-grid energy used by the heat pump (extracting heat from the environment) is not limited as compared to the limited amount of irradiation on any particular day.

With a hot water draw-off of 31 MJ/d, the heat pump system used an average daily energy of **12.0 MJ/d**. Comparing this to the reference System at **38.5 MJ/d (10.7**

kWh/d) of grid energy, the heat pump unit achieved the desired hot temperature service with 31% of the power. As expected, this percentage was an improvement over the spring experiment with its smaller hot water draw-off.

3.3 Autumn – large draw-off

Stressing the systems even further, the large hot water draw-off scheme was retained for the autumn experiment. For the seasonal load factor (Table 1), the daily hot water draw-off was then increased to 36.9 MJ/d (Table 6).

Table 6. Experiment summary: autumn – large draw-off.

Experiment period (Exp011)			Autumn: 9–22 April 2022 (14 days)		
Load/hot water energy draw-off			Large: 36.9 MJ/d		
System	**Lower element**		**Upper element**		**Comments**
	Temperature	Source	Temperature	Source	
1. REFUsol	70°C	Solar panels	60°C	Electricity grid	
2. Sun Flux	70°C	Solar panels	60°C	Electricity grid	
3. Easy Warm	70°C	Solar panels	Not connected		No grid power window defined
4. Heat pump	60°C				
5. Reference	60°C		Not connected		

3.3.1 Autumn irradiance results

The solar energy supply during the autumn experimental period is significantly reduced as compared to the summer period (Figure 21). The average irradiance during our autumn experiment was somewhat larger compared to the long-term NIWA average. The daily average irradiance was recorded at 3.2 kWh/m² for our experiment in comparison to the historical 2.7 kWh/m² NIWA average. Thus, the experimental conditions were more advantageous. The autumn performance of the solar systems would be reduced by more representative irradiation conditions.

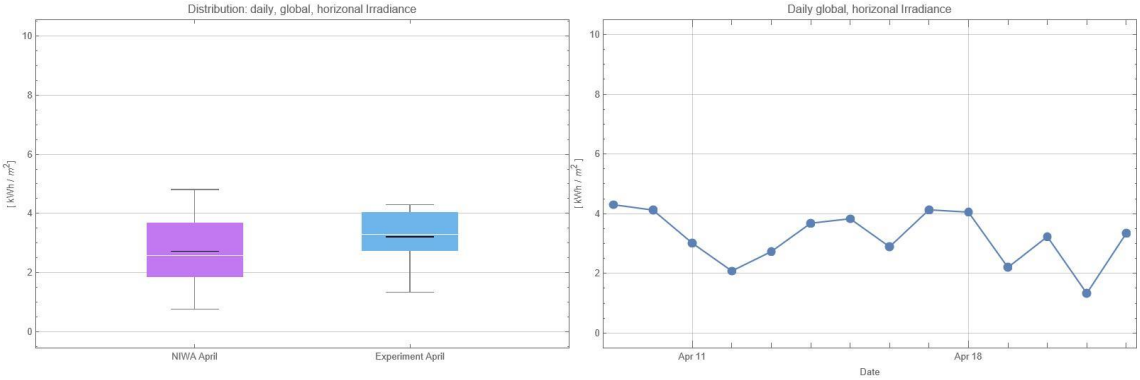

Figure 21. Irradiance for autumn experiment.

As the next sections show, the combination of significantly reduced solar energy supply while retaining the large water draw-off schedule was reflected in the performance of all three PV systems during the autumn experiment.

3.3.2 Autumn comparison: 1. REFUsol to 5. Reference

The top two cylinder volumes do not drop below 50°C for this experimental set-up. The daily average hot water draw-off was measured at 37.4 MJ/d, close to the nominal value. The average daily energy supplied by the PV panels to the unit was 23.1 MJ/d, while the energy from the grid to boost the upper element was **19.2 MJ/d**. (The value was corrected upwards by 0.3 MJ/d to make up for lower total energy in the cylinder at the end of the experiment.)

The reference System had a very similar draw-off of 37.5 MJ/d with a daily average energy consumption of **46 MJ/d**. Thus, the REFUsol system required 42% grid electricity compared to the reference system.

3.3.3 Autumn comparison: 2. Sun Flux to 5. Reference

The top two cylinder volumes did not drop below 50°C for this experimental set-up. The daily average hot water draw-off was measured at 37.5 MJ/d, close to the nominal value. The average daily energy supplied by the PV panels to the unit was 12.9 MJ/d, while the energy from the grid to boost the upper element was **30.2 MJ/d**.

The reference system had a very similar draw-off of 37.5 MJ/d with a daily average energy consumption of **46 MJ/d**. Thus, the Sun Flux required 65% grid electricity compared to the reference system.

Looking closer at the two simple PV system again, Figure 22 shows the necessary grid energy needed as a function of the solar irradiance conditions. There is now a much closer correlation between irradiation and grid power consumption, as the large draw-off (in the context of lower irradiance values) cannot be covered mostly by the PV systems.

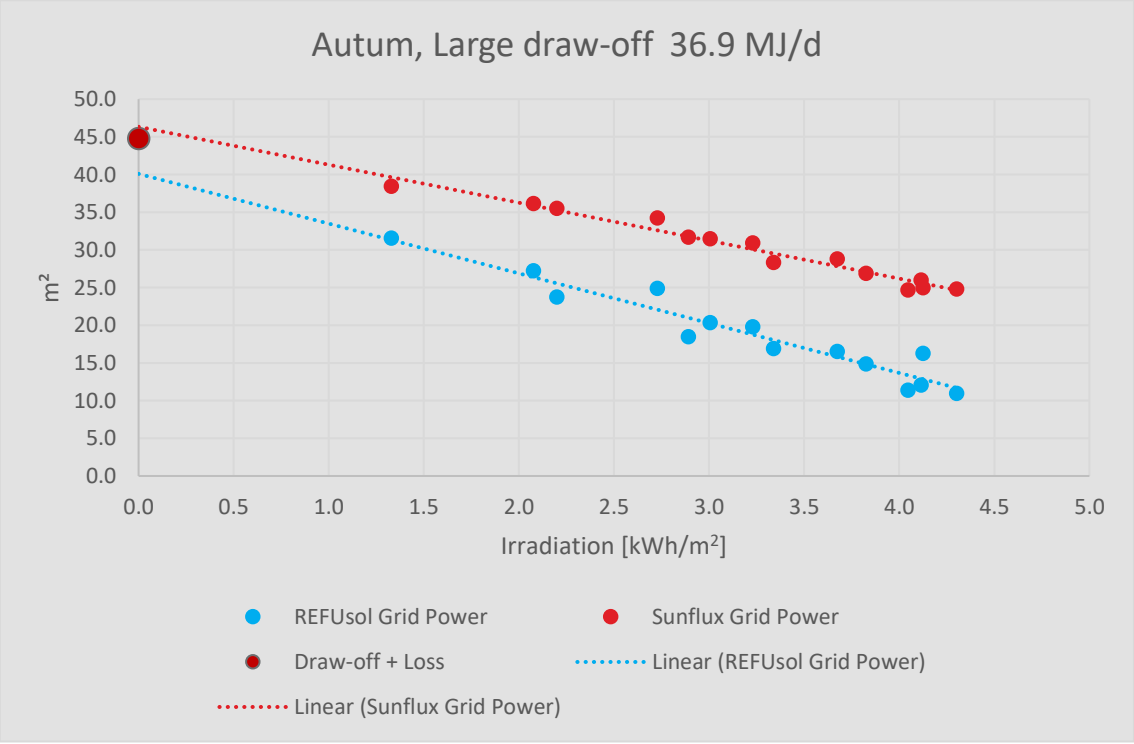

Figure 22. REFUsol and Sun Flux grid energy consumption as function of irradiance – linear fit is a guide to the eye only.

3.3.4 Autumn comparison: 3. Easy Warm to 5. Reference

During the spring and summer periods, the Easy Warm system with its largest PV array was largely able to cover the hot water needs (plus standing losses) without any grid electricity input. This was not the case during the autumn period, as expected. With an average daily energy demand of approximately 44.8 MJ/d (draw-off and losses – the reference system used 46 MJ/d) and a measured average daily solar generation of 38.7 MJ/d, the difference of approximately 6–8 MJ/d (1.6–2.2 kWh/d) would be required from the grid.

The option of using the grid electricity input was briefly explored at the end of the autumn experimental period. Two time windows of 30 minutes where defined where the heater element was powered by the grid instead of the solar array. The morning period was 7:00–7:30 and the afternoon period 16:30–17:00.

Figure 23 shows the temperatures with the additional grid electricity windows on a sunny day. The morning energy boost lifted the temperature of the bottom two water volumes to around 40°C. The afternoon window lifted the bottom-most water volume to around 70°C. However, by this stage, the cylinder had been heated as a whole by the significant solar energy input during the day.

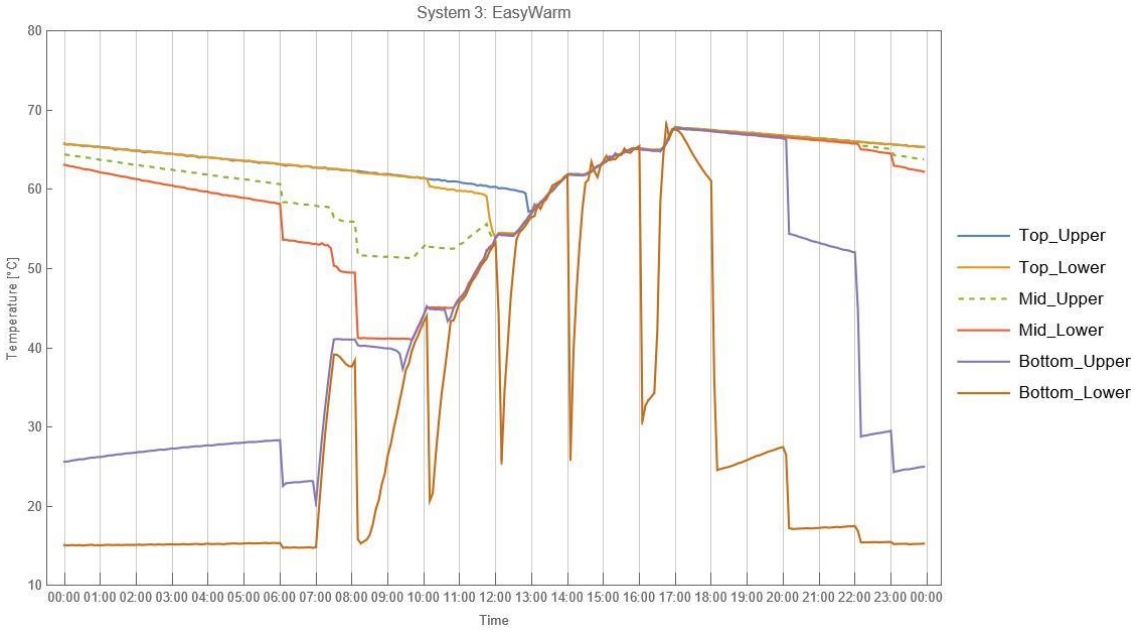

Figure 23. Easy Warm system with additional grid power – sunny day.

The picture was different on the following day with minimal solar irradiance (0.37 kWh/m²/d) available. Figure 24 shows again the grid electricity heating the bottom part of the cylinder to 40°C. However, the 30-minute window in the morning was not long enough to heat the whole cylinder to a level where it could cope with the large water draw-off during the day. The temperature of the upper-most volume dropped to around 30°C only by the end of the day. To avoid this, the grid electricity time windows would have to be enlarged significantly or the manual boost mode would need to be activated. However, enlarging the grid input windows would likely reduce the amount of energy sourced by the PV system on sunny days. Without frequent user intervention, the rigidity of defining these grid windows makes it challenging to achieve a system working at its optimum.

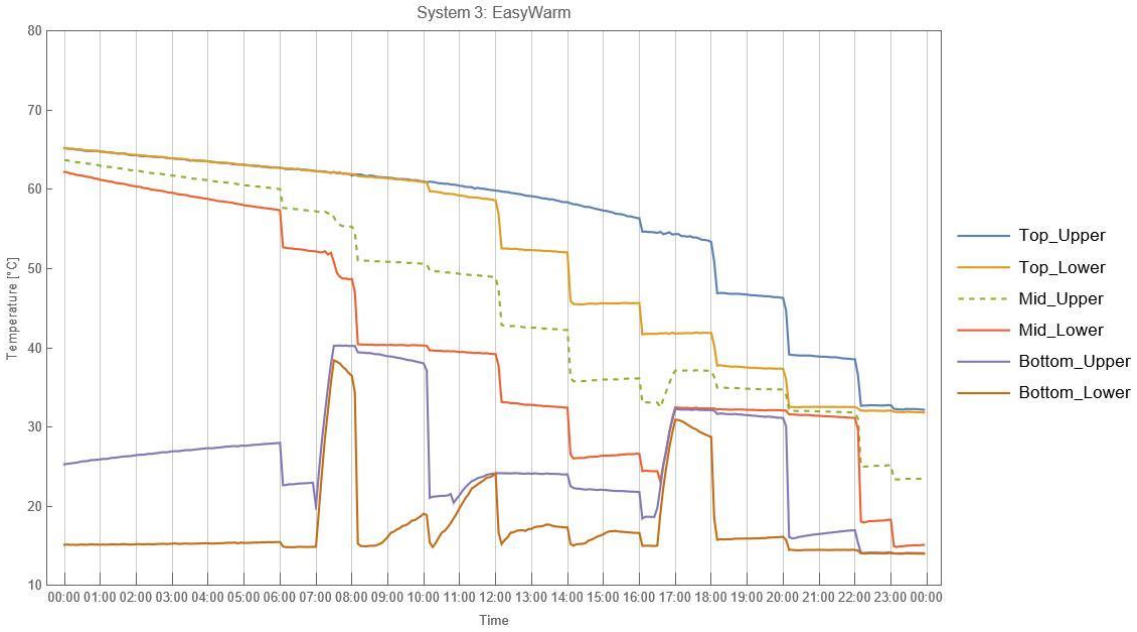

Figure 24. Easy Warm system with additional grid power – overcast day.

3.3.5 Autumn comparison: 4. Heat pump to 5. Reference

The daily average hot water energy draw-off for the heat pump system was measured as 37.9 MJ/d, which is close to the 36.9 MJ/d and the draw-off measured for the reference system (37.5 MJ/d). The grid electricity needed to achieve this was measured to be **16.5 MJ/d**, which was approximately 36% of the **46.0 MJ/d** required by the reference system.

3.4 Winter – small draw-off

For the winter experiment, we returned to the more realistic small draw-off scheme. The seasonal load factor (Table 1) was 1, which meant the nominal daily hot water draw-off was 25.6 MJ/d – slightly higher than the small load during the spring experiment. The Easy Warm system had been set up to utilise the grid power by defining two daily time windows where the heater element was switched over from the PV panels to the grid. All other parameters were unchanged (Table 7).

Table 7. Experiment summary: winter – small draw-off.

Experiment period (Exp013)			Winter: 23 June – 6 July 2022 (14 days)		
Load/hot water energy draw-off			Small: 25.6 MJ/d		
System	**Lower element**		**Upper element**		**Comments**
	Temperature	Source	Temperature	Source	
1. REFUsol	70°C	Solar panels	60°C	Electricity grid	
2. Sun Flux	70°C	Solar panels	60°C	Electricity grid	
3. Easy Warm	70°C	Solar panels/ grid power	Not connected		Two daily grid power windows: 04:30–05:30 and 16:00–17:00
4. Heat pump	60°C				
5. Reference	60°C		Not connected		

3.4.1 Winter irradiance results

The solar energy supply during the winter experimental period was further reduced compared to the autumn campaign. Figure 25 shows again the statistical distribution as box whisker plots for the long term NIWA data of July and June and for our experiment. The daily values for the 14-day experiment are given on the right. The mean daily irradiance value for our experiment was 1.65 kWh/m². This compares to the long-term NIWA data of 1.4 kWh/m². On two consecutive days, the solar energy supply was very low, with a minimum of 0.11 kWh/m² on 28 June 2022.

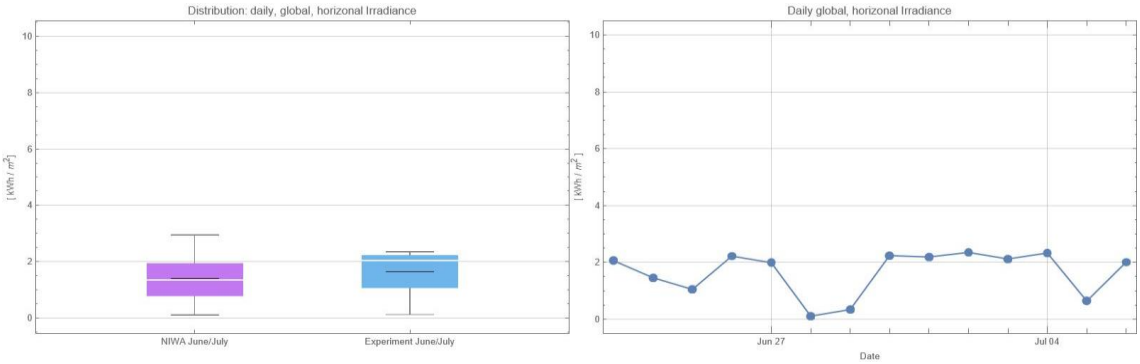

Figure 25. Irradiance for winter experiment.

3.4.2 Winter comparison: 1. REFUsol to 5. Reference

The REFUsol system met the criterion of not having the top two cylinder volumes drop below 50°C at any time during the experiment. The daily average hot water draw-off was measured as 26.5 MJ/d. The daily average energy provided by the PV array was 14.9 MJ/d while the daily average grid energy was **17.1 MJ/d**. This compares to an average daily energy demand of **35.1 MJ/d** for the reference system to provide the measured hot water draw-off of 25.8 MJ/d in addition to the standing losses. Consequently, the REFUsol system still only required approximately half of the grid energy that the reference systems used.

3.4.3 Winter comparison: 2. Sun Flux to 5. Reference

The Sun Flux system met the criterion of not having the top two cylinder volumes drop below 50°C at any time during the experiment. The daily average hot water draw-off was measured as 25.8 MJ/d. The daily average energy provided by the PV array was 6.9 MJ/d while the daily average grid energy was **25.2 MJ/d**.

3.4.4 Winter comparison: 3. Easy Warm to 5. Reference

The Easy Warm system met the criterion of not having the top two cylinder volumes drop below 50°C at any time during the experiment. The daily average hot water draw-off was measured to be 26.7 MJ/d with PV energy generated by the panels of 19.3 MJ/d. The two daily grid electricity boosts averaged to **18.1 MJ/d**. As mentioned, higher electrical losses are associated when converting the PV DC output to the AC current. It is noteworthy that the Easy Warm system with only one heater element at the bottom heated a larger water volume than the upper booster elements of the REFUsol and Sun Flux systems. Consequently the average stored energy in the Easy Warm system was significantly higher (331 MJ) as compared with the REFUsol (316 MJ) and Sun Flux (313 MJ) systems. With this water-draw-off schedule, the consumer would not benefit from this higher stored energy. This is similar to the reference system with its lower element and a very homogeneous energy content of 333 MJ.

3.4.5 Winter comparison: 4. Heat pump to 5. Reference

The heat pump system delivered an average daily hot water draw-off of 25.9 MJ/d. The grid energy needed to achieve this was measured as **16.1 MJ/d**. This was approximately 46% of the energy needed by the reference system.

Figure 26 compares the heat pump system to the reference system across all four seasons. The relation between grid electricity and hot water draw-off exhibits a linear dependency with a y-axis intercept indicating the standing losses. The slope of this relationship is lower for the heat pump as expected. This also underlines the advantage of a heat pump system relative to the conventional system as the hot water draw-off requirement increases. The heat pump data exhibits more scatter around a linear relation compared to the reference system likely caused by changes in efficiency of the system as the outside temperature changed over the seasons.

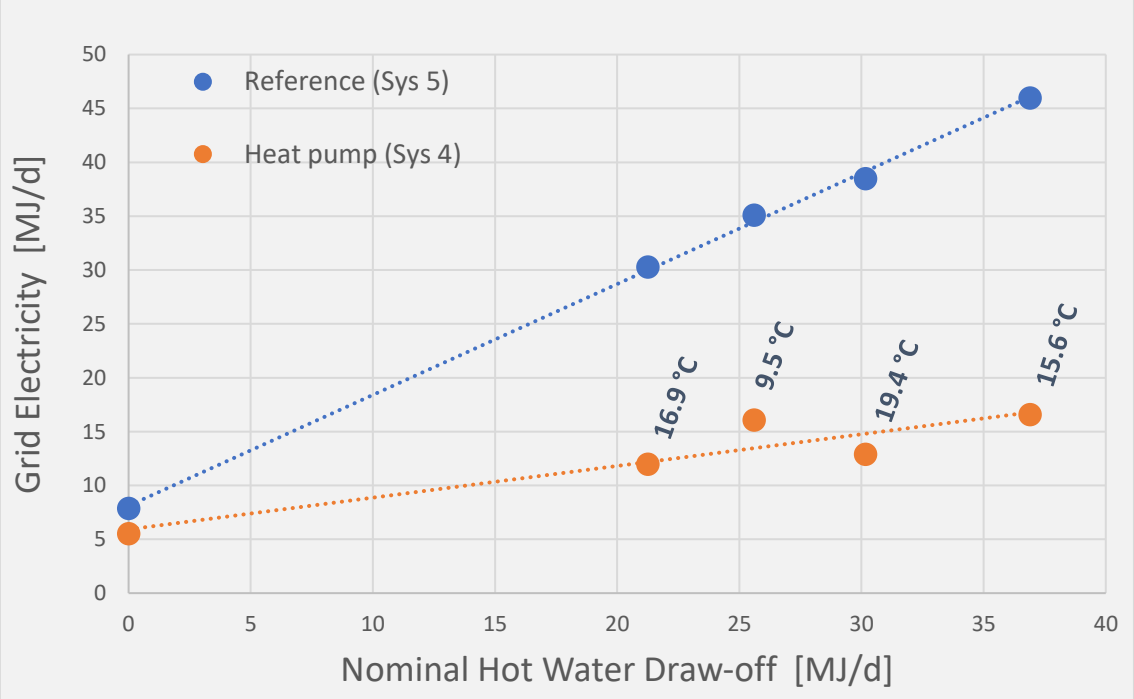

Figure 26. Comparison between heat pump system and reference system – average outside temperatures given.

Interestingly, the fingerprint of the scatter is similar in nature for the reference system. The standing losses of the reference system are also impacted by the ambient temperature.

3.5 Overall summary of results

Table 8 provides a summary of the grid energy requirements for each of the season/size tests for the REFUsol, Sun Flux and Reclaim Energy CO_2 heat pump systems. The Easy Warm system is not included in this summary as the wintertime boosting between the small and large draw-offs was not done in a consistent way so the results are difficult to interpret. The size of the systems vary so care must be taken when comparing values between systems within this table.

Table 8. Comparison of grid energy requirements for the various experiments.

Scenario/season	System[9]	Grid electricity required (MJ/d)	Percentage of reference system
Small/summer (spring)	1. REFUsol	3.4	12%
	2. Sun Flux	10.6	33%
	4. Heat pump	12.0	40%
Small/winter	1. REFUsol	17.1	57%
	2. Sun Flux	25.2	84%
	4. Heat pump	16.1	46%
Large/summer	1. REFUsol	1.8	5%
	2. Sun Flux	13.0	34%
	4. Heat pump	12.9	43%
Large/winter (autumn)	1. REFUsol	19.2	42%
	2. Sun Flux	30.2	66%
	4. Heat pump	16.5	36%

The data from Table 8 is represented in graphs in Figure 27 and Figure 28. These show the size of reference system draw-offs along with grid energy requirements (shown in brown and dark blue). The remainder of the energy requirements reflect how various systems performed. Of note is the small summertime grid energy requirements for the REFUsol system while the heat pump system had more consistent grid energy requirements for summer and winter. Grid energy requirements for systems 1, 2 and 4 are shown as a darker shade (brown for summer, dark blue for winter) with the difference (advantage provided by the system) given as the lighter colour at the bottom (yellow for summer and light blue for winter).

[9] The early experiments on the Easy Warm system did not have a grid connection boost window set and consequently the cylinder was often colder than the acceptable conditions. The Easy Warm system was excluded from this table for this inconsistent configuration.

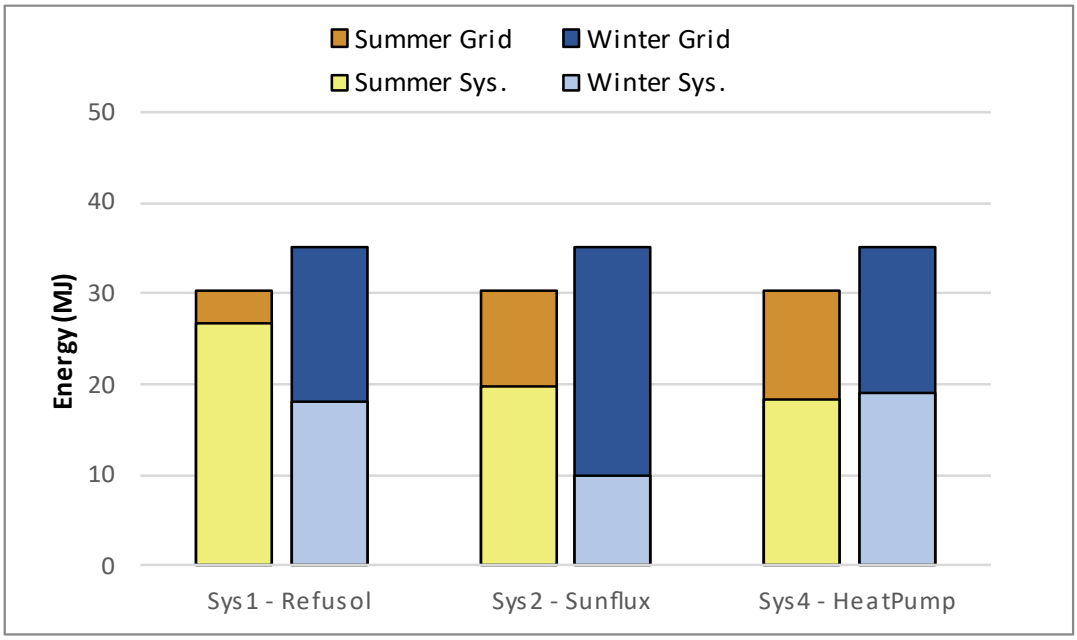

Figure 27. Summer and winter reference system grid energy requirements – small draw-offs.

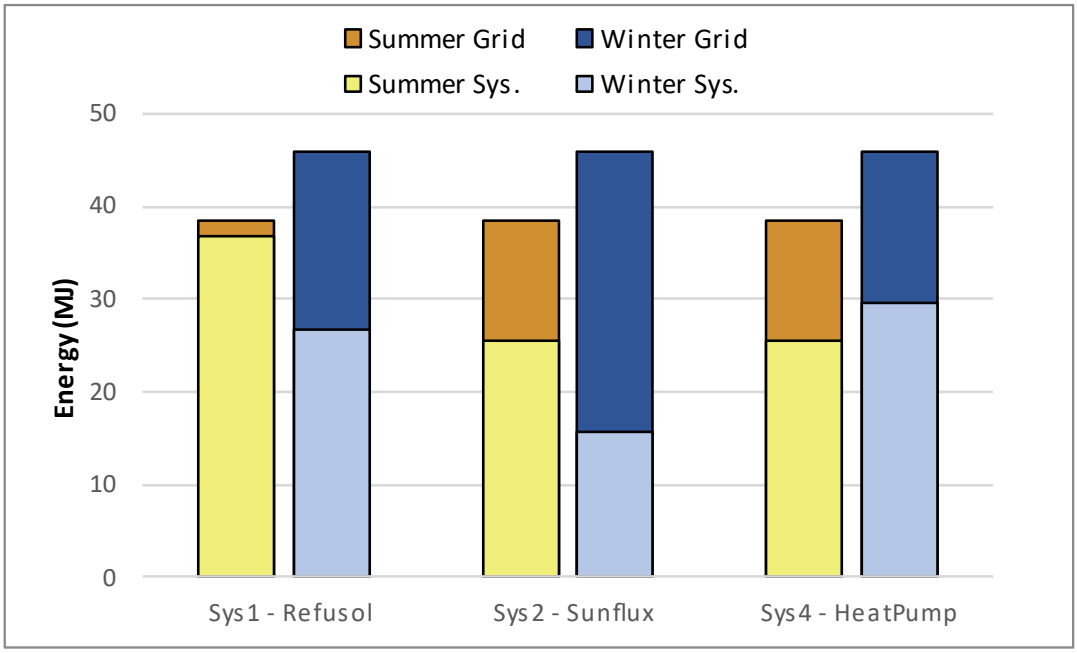

Figure 28. Summer and winter reference system grid energy requirements – large draw-offs.

4. Discussion and conclusions

Water heating is estimated to use around 31% of residential energy in New Zealand homes (Energy Consult, 2020). All of the systems examined in this report were effective in reducing the grid electricity required to provide for the hot water demand when compared to the reference system, but the savings varied depending on the system, the season and the draw-off scenario. The grid electricity requirements are summarised in Table 8 and shown in Figure 27 and Figure 28.

The REFUsol and Sun Flux systems (small direct PV) provided supplementary heating that would clearly need additional grid electricity resistive heating to provide for the household's water heating needs throughout the year. These systems reduced grid electricity requirements by between 16% and 95% depending on the season and draw-off scenario.

The larger direct PV unit (the Easy Warm system) was an effective complete water heater replacement. The unit also provided specific control of the supplementary heating, which would allow homeowners to tune their use of the system to minimise the supplementary heating requirement.

The CO_2 heat pump water heater system also outperformed the reference system, and the performance was less seasonally dependent than the solar systems, requiring 54–64% of the grid electricity requirements of the reference system. During winter when the solar systems often required supplementary heating from the electric resistance heating, the heat pump water heater continued to operate, requiring only modest overall electrical input. However, in summer when the solar systems were often able to fully meet the water heating needs with solar input alone, the heat pump water heater still required a modest electrical input.

A heat pump system provides a convenient solution for those who wish to reduce their water heating energy requirements even when their access to solar energy is limited. However, a CO_2 heat pump water heater system is more expensive than the other systems – a factor that would need to be considered in any cost-benefit analysis.

In contrast to the heat pump system and the reference system, both of which use only grid electricity, the direct PV systems were intended to channel as much solar energy into the hot water system as possible to offset as much of the conventional grid electricity-based water heating as possible.

In this respect, the Sun Flux system was the smallest and most basic of the direct PV systems and provided around two-thirds of the water heating needs in summer and one-third in winter. For such systems, the use of dual elements makes sense so that the direct PV system is connected to the lower heating element allowing for the capture of solar energy at the bottom of the cylinder. The upper element can then be used to provide for the required supplementary heating for the system.

The REFUsol system provides slightly more solar collection and has an improved controller (including MPPT). The solar contribution to the water heating in summer was around 88–95% while around 43–58% was still possible in winter. This system seems to be well positioned, with sufficient solar collector area while still having a low-cost, basic controller.

The Easy Warm system further increases the area of solar collectors within the system and the controller is further improved with the use of a modified inverter that has a sine output. This system fully controls the bottom element of the cylinder and could be readily retrofitted to an existing hot water cylinder. The Easy Warm system was able to provide for all of the summer water heating demands for both the large and small sized loads but did require supplementary heating for the winter tests. The controller for the Easy Warm system defined windows for when grid energy could be fed into the system but this was not optimised and varied in how it was applied among the different configurations within the experiments. Consequently, it is difficult to compare the Easy Warm system with the other systems.

The PV water heating systems in this report (all direct PV) have focused on getting solar energy directly into the water as easily as possible with a minimum of equipment and cost. As the use of conventional household PV systems has become more common, more electricity generated from PV could potentially be directed into hot water systems, which is the basis of diverter systems and outside the scope of this report.

The design and optimisation of these systems is complicated, but there would be a benefit to ensuring that low-cost energy storage solutions in the form of heated water in hot water cylinders are included in preference to more costly energy balancing options such as expensive on-site batteries or trading electricity with the retailer at unfavourable rates.

The economic costs and benefits of these systems are subject to a number of assumptions that would require further exploration.

References

Apricus. (n.d.). *How combining PV solar with a CO_2 heat pump will save you money.* www.ecohotwater.co.nz/how-combining-pv-solar-with-a-co2-heat-pump-will-save-you-money/

Dortans, C., Anderson, B. & Jack, M. (2019). *NZ GREEN Grid household electricity demand data*. University of Otago. https://ourarchive.otago.ac.nz/esploro/outputs/report/NZ-GREEN-Grid-Household-Electricity-Demand/9926481772301891

EECA. (2020). *Ripple control of hot Water in New Zealand*. https://www.eeca.govt.nz/assets/EECA-Resources/Research-papers-guides/Ripple-Control-of-Hot-Water-in-New-Zealand.pdf

EECA. (2021). *Hot water systems discussion paper: Comparative technology method for evaluating the performance of hot water systems*. Equipment Energy Efficiency (E3) Program. https://www.energyrating.gov.au/sites/default/files/2022-12/e3-hot-water-discussion-paper-comparative-technology-method.pdf

EECA. (2023). *Sales & efficiency data.* https://www.eeca.govt.nz/insights/eeca-insights/e3-programme-sales-and-efficiency-data/

EnergyConsult. (2020). *RBS2.0 methodology report.* Department of Industry, Science, Energy and Resources. https://www.energyrating.gov.au/sites/default/files/2022-12/2021_rbs_methodology_report.v1.3.pdf

Isaacs, N., Camilleri, M., Burrough, L., Pollard, A., Saville-Smith, K., Fraser, R., Rossouw, P., & Jowett, J. (2010). *Energy use in New Zealand households: Final report on the Household Energy End-Use Project (HEEP)* (BRANZ Study Report SR221). BRANZ Ltd. https://www.branz.co.nz/pubs/research-reports/sr221/

Kasten, F., & Young, A. T. (1989). Revised optical air mass tables and approximation formula. Applied Optics, 28(22), 4735–4738. https://doi.org/10.1364/AO.28.004735

Meinel, A B., & Meinel, M. P. (1976). *Applied solar energy. An introduction*. Addison-Wesley.

Pollard, A. (2010). *The energy performance of heat pump water heaters* (BRANZ Study Report SR 237). BRANZ Ltd. https://www.branz.co.nz/pubs/research-reports/sr237/

SolarQuotes. (2017, August 25). *Sun Flux review: Hot water with dedicated solar PV panels*. https://www.solarquotes.com.au/blog/sun-flux-review-hot-water-with-dedicated-solar-pv-panels/

Stats NZ. (2023, July 10). *Dwelling and household estimates: June 2003.* https://www.stats.govt.nz/information-releases/dwelling-and-household-estimates-june-2023-quarter/

Turner, L. (2023, April 4). *Direct PV solar hot water buyers guide*. https://renew.org.au/renew-magazine/all-electric/direct-pv-solar-hot-water-buyers-guide/

White, V. (2020). *Assessing the condition of New Zealand housing: Survey methods and findings* (BRANZ Study Report SR456). BRANZ Ltd. https://www.branz.co.nz/pubs/research-reports/sr456-assessing-condition-new-zealand-housing-survey-methods-and-findings/

Appendix A: Irradiance on arbitrary surfaces

The time-dependent global irradiance E_{global} (direct solar beam and diffuse radiation measured in [W/m²]) incident onto the solar panels is needed to estimate the energy yield of the PV arrays during the planning stage. Once the system is installed, it is required for quality control – does the system deliver the anticipated energy yield? In this appendix, we present formulae to estimate the clear-sky irradiance for any given location and orientation of the solar array. The second part of the appendix deals with converting the measured irradiance of a horizontal pyranometer to that of a tilted surface. The angular position of the sun at a geographical location and any given point in time is readily available using commercial software packages such as Wolfram Mathematica.[10] Figure 29 shows the coordinate system used.

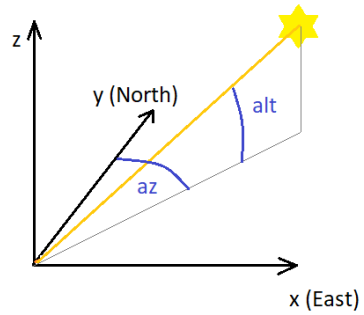

Figure 29. Definition of axes and angles.

The spherical coordinates (azimuth and altitude) can be transformed to the cartesian coordinates x, y, z using:

$$x = \cos(alt) \cdot \sin(az)$$

$$y = \cos(alt) \cdot \cos(az)$$

$$z = \sin(alt)$$

A1. Estimated irradiance on a tilted surface

To estimate the irradiance onto an arbitrary tilted and oriented surface such as a PV panel, it is easier to convert the position of the sun, usually expressed as angles of azimuth and elevation, to vectors. The dot product between the time-dependent incident solar unit vector $\overrightarrow{S(t)}$ and the normal to the surface of the solar panel (unit vector $\overrightarrow{N}$) will yield the reduced energy yield onto this tilted surface. The solar incident vector $\overrightarrow{S(t)}$ is multiplied with the irradiance scalar E_i, which is the energy flux perpendicular to the solar incident vector $\overrightarrow{S(t)}$.

$$E_{module} = E_i \, \overrightarrow{S(t)} \cdot \vec{N}$$

The direct component of the incident irradiation E_i is described by the experimentally determined equation (Meinel & Meinel, 1976):

$$E_i = 1353 \times 0.7^{AM^{0.678}}$$

[10] www.wolfram.com/mathematica

where the value 1,353 W/m² is the solar constant and *AM* is the angle-dependent air mass factor. This factor describes the reduction of light as it passes through the atmosphere and is absorbed by air molecules and dust. Kasten and Young (1989) give an equation for *AM* considering the curvature of the atmosphere:

$$AM = \frac{1}{\cos(\theta) + 0.50572(96.07995 - \theta)^{-1.6364}}$$

where θ is the angle between the vertical and the direction of the sun. This equation is used in the calculation of $E_{i,}$. The value of 0.7 in this relation arises from the fact that only about 70% of the radiation incident on the outer atmosphere is transmitted to the surface of the Earth. From our own experimental irradiance data, a factor of 0.75 describes the data more accurately, which is therefore used in our calculations.

Even on a clear day, the diffuse radiation will add approximately 10% of the direct irradiance on a given surface. Thus, the global irradiance is estimated as:

$$E_{global} = 1.1\, E_i$$

Figure 30 shows the calculated irradiance values for a horizontal surface and a surface tilted by 16° for the BRANZ site on 21 January 2020. Also given are the measured irradiance levels for a horizontal surface. A good agreement between the calculated and the measured values is achieved.

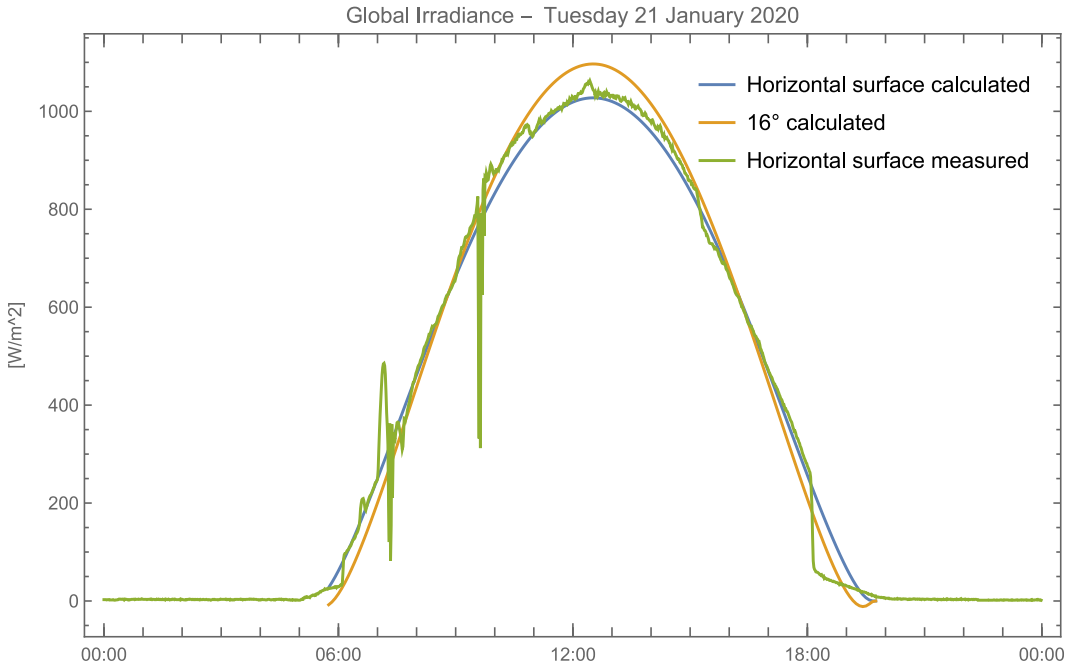

Figure 30. Irradiance measured and calculated on the horizontal surface as well as the irradiance calculated for the 16° surface.

A2. Conversion of horizontal measurement data to tilted surfaces

In our case, the global irradiance is measured using a pyranometer mounted horizontally in close proximity to the solar array. Our instrument measures the direct irradiance as well as the diffuse part of the global irradiance. To determine the solar energy received by the solar panels installed at a 16° angle, the measured direct irradiance is corrected as follows (Figure 31):

$$E_{16°}(t) = \frac{\overrightarrow{S(t)} \cdot \vec{N}}{\overrightarrow{S(t)} \cdot \vec{H}} E_{horiz,meas}(t)$$

where:

$E_{16°}(t)$	is the resulting, corrected direct irradiance for the tilted surface of the solar panels
$E_{horiz,meas}(t)$	is the direct irradiance measured in the horizontal plane
$\overrightarrow{S(t)} \cdot \vec{N}$	is the dot product of the time dependent solar incident unit vector $\overrightarrow{S(t)}$ and the unit normal vector $\vec{N}$ to the solar panels
$\overrightarrow{S(t)} \cdot \vec{H}$	is the dot product of the time-dependent solar incident unit vector $\overrightarrow{S(t)}$ and the unit normal vector $\vec{H}$ to the horizontal surface (plane of pyranometer measurement). The latter only has a z-component and thus the dot-product reduces to the sine of the sun elevation angle: sin*(alt).* Dividing the measured direct irradiance $E_{horiz,meas}(t)$ by sin*(alt)* is then simply the direct incident irradiance E_i .

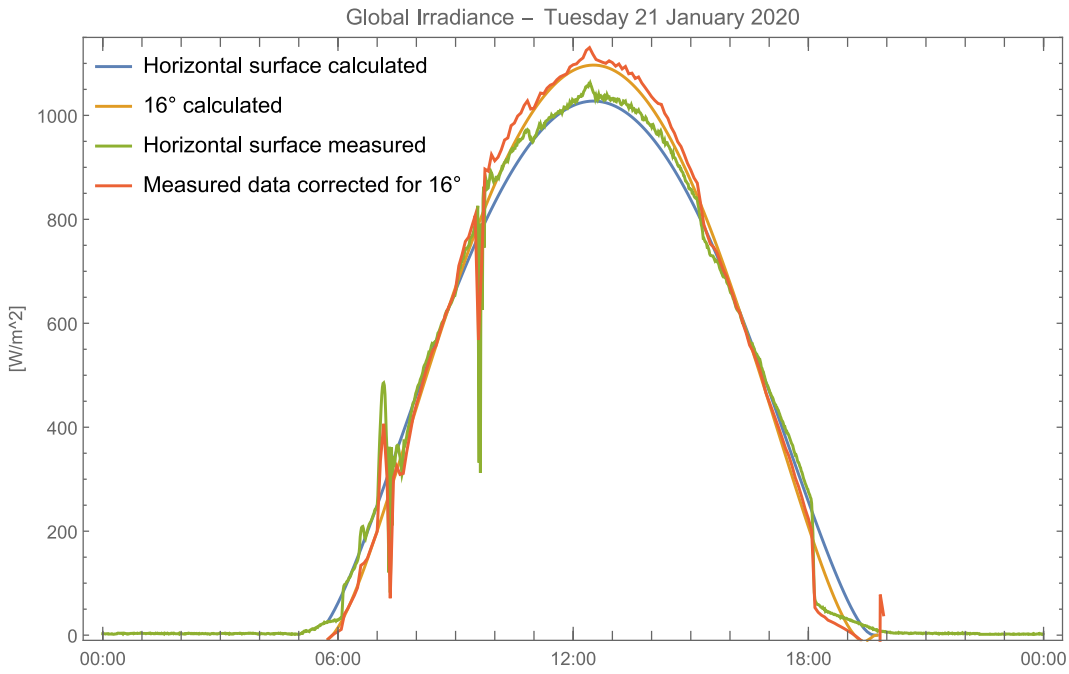

Figure 31. Irradiance measured and calculated on the horizontal surface, irradiance calculated for the 16° surface and the measured irradiance data corrected for the 16° surface.

Appendix B: PV system commissioning

The performance of the PV panels in combination with the three heating units depends on many factors and can be challenging to evaluate in detail. The voltage-current curve of PV panels is not linear and strongly dependent on the irradiation conditions as well as temperature of the panels. The maximum electrical generation at the so-called maximum power point (MPP) is also highly variable. To ascertain that the systems perform as expected, a number of commissioning evaluations have been performed under load conditions, thus moving beyond simply recording open-circuit voltage V_{oc} and short-circuit current I_{sc}. Table 9 gives the manufacturer's specification for the PV panels.

Table 9. Extended PV panel specifications.

Nominal power W_{peak}	315 W	Irradiance = 1,000 W/m²	
Nominal voltage V_{mpp}	33.9 V	Spectrum AM 1.5	
Nominal current I_{mpp}	9.31 A	T_{cell} = 25°C	
Open circuit voltage V_{oc}	40.5 V	Temperature coefficient V_{oc}	-0.27 %/°C
Short circuit current I_{sc}	10.09 A	Temperature coefficient I_{sc}	0.04 %/°C

The tests were performed during clear, sunny days with the cylinders cold to ensure that the full system power was employed for the whole day. The commissioning fell into autumn, so the irradiance did not reach the desired 1,000 W/m². However, the results can easily be scaled to lesser irradiances.

B.1 REFUsol

Figure 32 shows the DC voltage of one of the three strings of the REFUsol unit. Each of the three strings has two panels connected in parallel. The nominal V_{mpp} and V_{oc} values are given by the red lines. The measured voltage during operation is close to the V_{mpp} as expected, especially during the early morning and late afternoon hours. During midday, the voltage drops slightly, which is consistent with the temperature dependence of the solar cells. Assuming the panels reach their highest temperature during midday, a cell temperature of 45°C (nominal operating temperature) would result in a voltage reduction of 5.4%, reducing the V_{mpp} voltage from 33.9 V to around 32 V. This is reflected in the measurements.

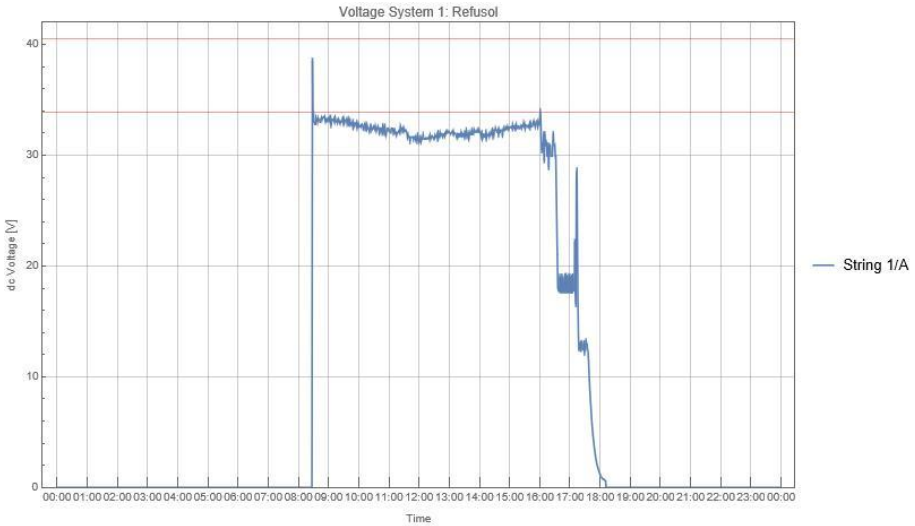

Figure 32. REFUsol voltage.

Figure 33 shows the corresponding current measured on one of the three REFUsol strings and calculated current based on measured irradiance. The maximum measured global irradiance (horizontal) was 470 W/m² shortly after midday. Assuming an I_{mpp} current that is proportional to the irradiance, the calculated (non-corrected, black) curve would be obtained for two panels in series. Correcting the irradiance for the 16° panel tilt, the light green graph is obtained, which is now close to the measured current. The spikes in the morning and evening are artefacts. Scaling the nominal I_{mpp} of 18.6 A at standard test conditions to the corrected irradiance of approximately 690 W/m² at midday, a current of 12.8 A would be expected in reasonable agreement with the 12.0 A measured. The other two strings behave similarly.

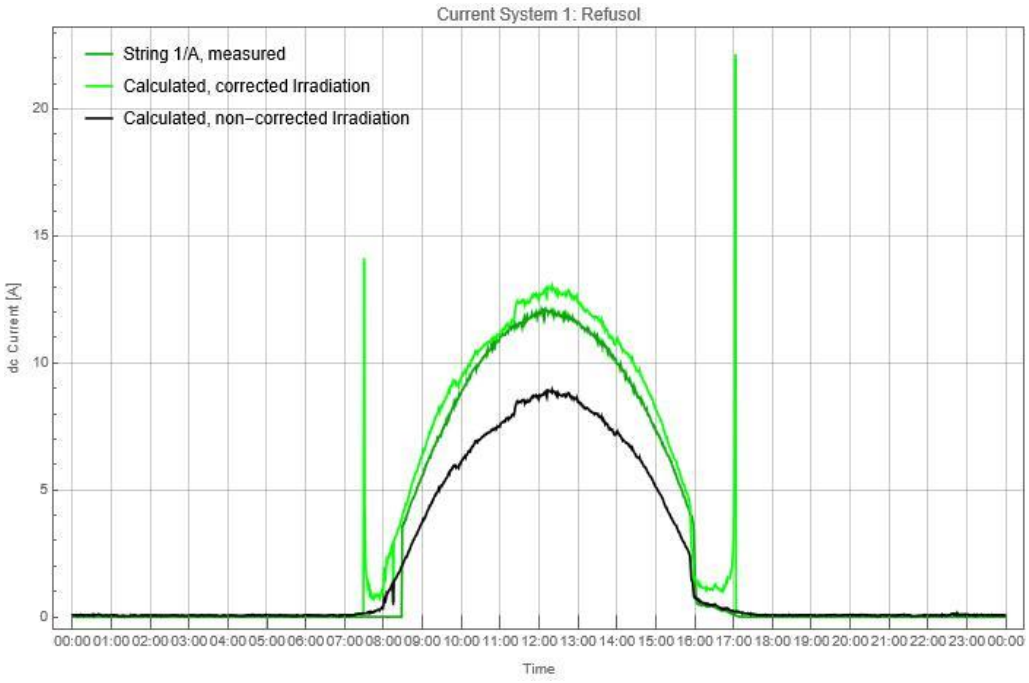

Figure 33. REFUsol current.

The nominal power output of one string at the peak irradiance, taking into account the reduced voltage due to temperature effects, would be approximately 32 V · 12.8 A = 410 W as compared to the 380 W measured (due to the reduced current). Taking into account cable losses can explain some of this difference. The conductor used is a 2 · 6 mm² core with an overall total length of approximately 16 m. Assuming a copper conductivity and 12 A / 30 V current, the electrical losses are of the order of 4%, reducing the gap between the nominal and actual power output to less than 20 W. Efficiency losses within the device are neglected here but would contribute to this.

The maximum power specification of the heater element is stated in the specification as 1,500 W – 500 W for each of the three strings powering one of the three interwoven elements. Where there is more solar irradiance available with potentially larger power output into the system, the unit limits its output. Figure 34 shows this limitation to 500 W on a sunny day[11] between 9:00 and 16:00. In addition to the power limitation, the graph shows frequent periods of time where the system doesn't deliver any energy to the cylinders as the maximum set temperature is achieved.

[11] Peak irradiance perpendicular to the panel was approximately 1,250 W/m².

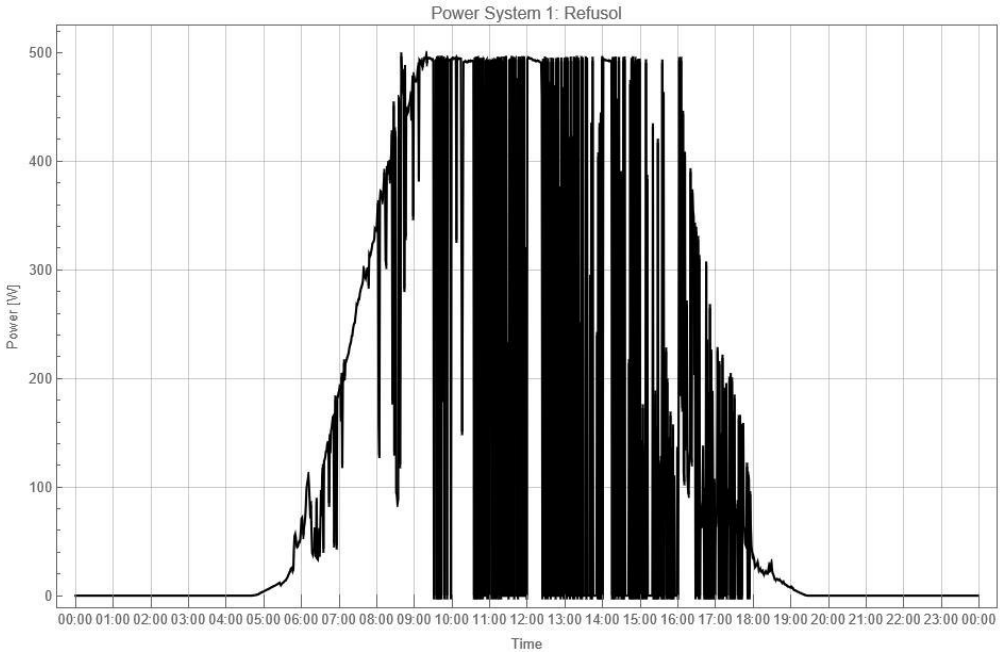

Figure 34. REFUsol unit limiting the power output to 500 W per element.

In summary, the electrical parameters of the strings connected to the REFUsol unit with its maximum power point trackers are close to what is expected.

B.2 Sun Flux

Figure 35 shows the measured voltage of the Sun Flux system with its four panels connected in series on 19 May 2021, which was a sunny autumn day with a peak irradiance of around 690 W/m² (for the tilted module plane). Again, the open circuit voltage V_{oc} and voltage and the maximum power point voltage V_{mpp} under standard test conditions are indicated by the red lines.

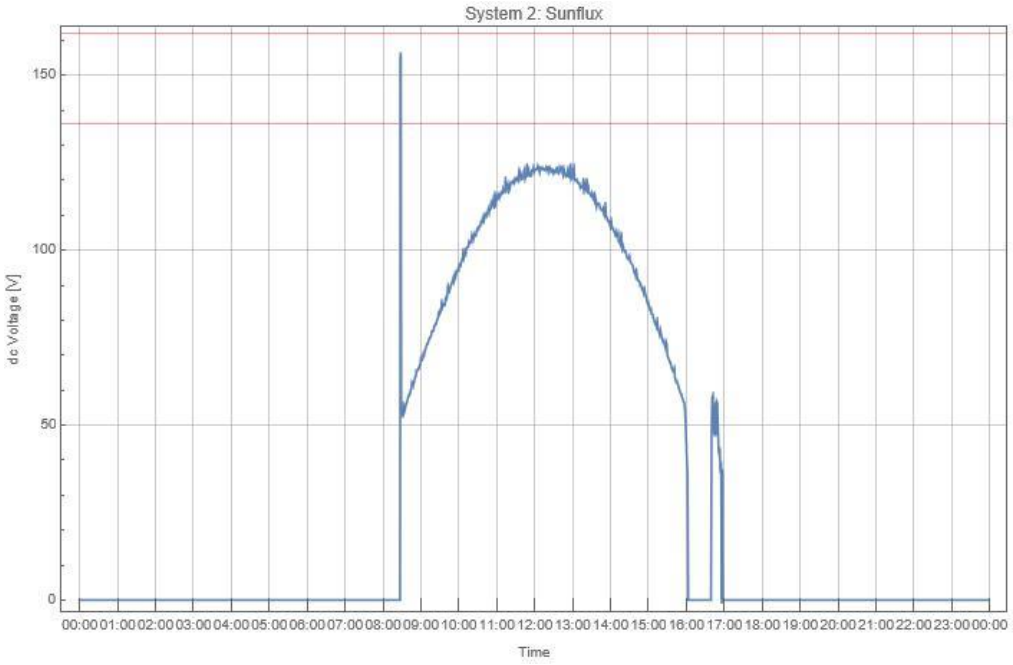

Figure 35. Sun Flux voltage.

Noticeable is different behaviour of the voltage in comparison to the REFUsol unit. While the REFUsol string voltage is fairly constant for all irradiance levels throughout the day, the Sun Flux graph looks much more like an inverse parabola. This indicates that the Sun Flux device does not use a maximum power point tracker. The voltage of a PV cell quickly approaches V_{oc} even under low-light conditions while the current is close to proportional to the irradiance. In case of the Sun Flux unit, the voltage increases gradually with an increasing irradiance, thus operating away from the maximum power point of the panels. Plotting the ratio of voltage over current for several hours in the morning gives resistance values (Figure 36) between 20 and 21 ohms, which is the resistance of the heating element at the hot cylinder temperature.

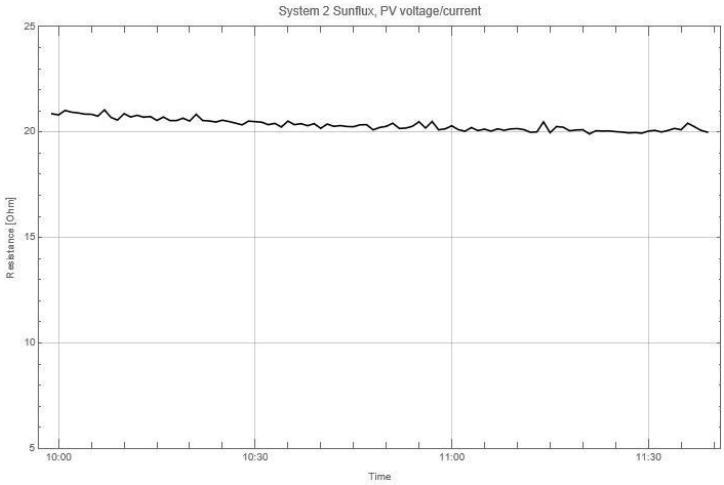

Figure 36. PV voltage/current.

Looking at the current, we find a good agreement between measured and calculated values. We use the measured horizontal irradiance corrected for a 16° tilt. Scaling the nominal STC current of 9.31 A to the irradiance gives a light green curve in very good agreement with the measured dark green data set (Figure 37).

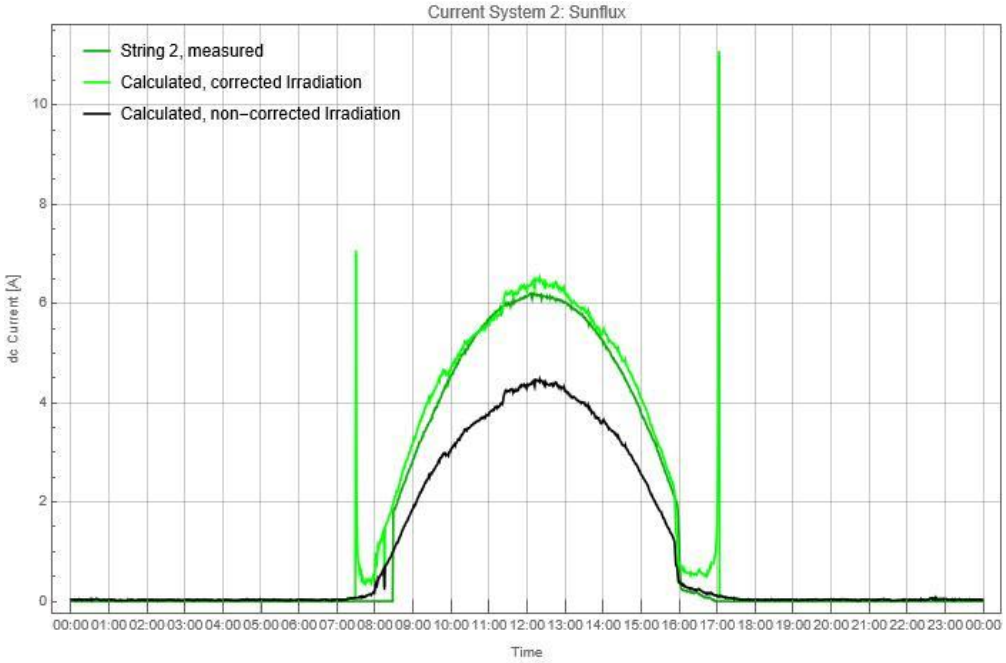

Figure 37. Sun Flux current at a peak irradiance (tilted panel) of around 690 W/m².

Assuming a voltage of the four panels closer to the V_{mpp} value (but also reduced by the temperature coefficient) and the measured current, a power output of 4 · 32 V · 6.4 A = 819 W would be obtained. This compares to the measured 764 W. The electrical losses in the cable are expected to be less than 1% and lower as compared to the REFUsol unit. The four panels are in series thus increasing the voltage with a lower current, which helps to keep the cable losses down. The larger performance gap is likely due to not tracking the maximum power point of the PV array.

Looking at a sunny spring day (25 November 2021) with irradiances on the tilted module surface of around 1,200 W/m², the disadvantages of not having an MPPT can be further illustrated. Figure 38 shows the Sun Flux current with maximum values of around 7.1 A, which is significantly below the optimal current output for this panel under these high irradiances.

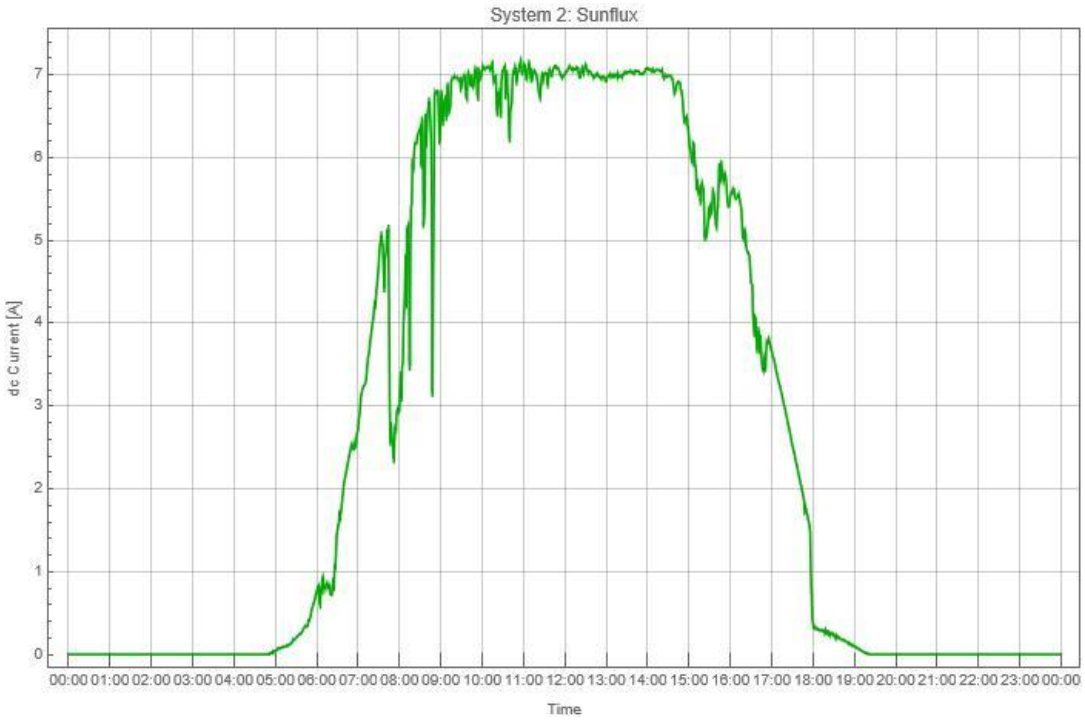

Figure 38. Sun Flux current at a peak irradiance (tilted panel) of around 1,200 W/m².

The explanation again lies in the non-linear I-V curve and the Sun Flux unit not being able to follow the maximum power point of the PV panels.

Figure 39 shows approximated I-V curves for irradiances between 1,200 W/m² and 500 W/m² for four modules in series together with the linear resistive element of 21 ohms. While the device operates close to the maximum power point for irradiances around 700–800 W/m² (the first Sun Flux example given above), for higher irradiances, such as the second example, this maximum power point is increasingly lost. The linear graph for the resistive element intercepts the I-V curve (1,200 W/m²) at around V = 155 V and I = 7.4 A. Bearing in mind the approximation of the I-V curves, this is in good agreement with the measured voltage and current.

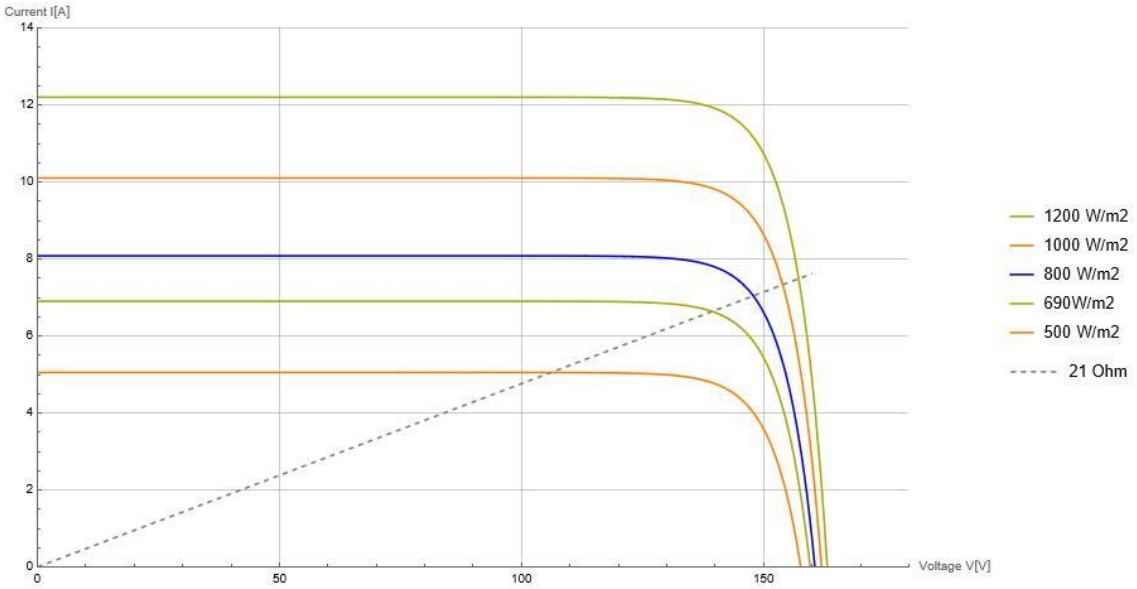

Figure 39. Theoretical I-V graphs for four panels connected in series and for different irradiance levels together with an ohmic resistive element of 21.

In summary, the Sun Flux unit operates as expected for a device without an MPPT.

Appendix C: Irradiance data

As mentioned in section 2.1.2, the irradiance is measured on site at BRANZ using two separate instruments giving very similar results. In addition, some long-term average irradiance data was needed to evaluate if our experimental results were obtained under representative irradiance conditions. Average data from NASA[12] and NIWA is given for Wellington in the table below.

The data is monthly averages for the daily energy sums per square metre (kWh/m²/day). The NASA monthly averages are calculated using the average of 37 years (1984–2020). The NIWA data is derived from its Typical Meteorological Year (TMY) data from the Kelburn, Wellington weather station (Table 10).

Table 10. Monthly mean of daily irradiance sums for Wellington.

kWh/m²/day	Jan	Feb	Mar	Apr	May	Jun	Jul	Aug	Sep	Oct	Nov	Dec
NASA	6.68	5.87	4.58	3.17	2.14	1.64	1.84	2.71	3.87	5.14	6.26	6.67
NIWA	6.58	5.47	4.10	2.71	1.77	1.36	1.44	2.34	3.46	4.75	6.24	6.40

[12] https://power.larc.nasa.gov/data-access-viewer/